Natural Hazards (2026) 122:461
https://doi.org/10.1007/s11069-026-08205-7

ORIGINAL PAPER

Unraveling Holocene surface-faulting history of the Çay segment, Sultandağı Fault (SSW Türkiye): linking paleoseismic evidence to segment-scale seismic behavior

Volkan Özaksoy[1] · Hasan Elmacı[2] · Hasret Ozan Avcı[2] · Mustafa Softa[3]

Received: 26 June 2025 / Accepted: 5 May 2026
© The Author(s) 2026

Abstract
The ~115 km long Sultandağı Fault forms the southern boundary of the Quaternary Afyon–Akşehir Graben in western Türkiye and represents a major active normal fault within the regional extensional regime. The Mw 6.5 Çay earthquake of 3 February 2002 produced surface rupture along its central segment, confirming its seismogenic capacity. This study presents the first detailed paleoseismological investigation of the Çay segment based on two trenches (Eskiköprü and Maltepe) excavated across faulted Holocene deposits. Stratigraphic and structural evidence documents five Holocene surface-rupturing earthquakes (E1–E5), including the historically documented 2002 Çay earthquake. Fourteen AMS radiocarbon samples (charcoal, bone, and carefully selected bulk organic sediments) were analyzed and modeled using a Bayesian approach in OxCal with stratigraphic constraints. Event ages and inter-event intervals were calculated at the 95.4% probability level (2σ), yielding millennial-scale recurrence behavior with uncertainty ranges extending up to ~1.59 kyr. The ~26 km cumulative surface rupture length observed during the 2002 earthquake corresponds to Mw≈6.7 based on the Wells and Coppersmith (1994) normal-fault scaling relation, consistent with instrumental estimates. Measured vertical displacements (~20–25 cm) in trench exposures support moderate-magnitude (Mw 6–7) earthquake potential for single-segment ruptures. These results demonstrate repeated Holocene surface faulting with millennial recurrence intervals and confirm the capacity of the Çay segment to generate Mw≥6.5 earthquakes. The findings provide quantitative input for time-dependent seismic hazard assessment within the Akşehir-Simav extensional system.

Keywords Sultandağı Fault · Çay segment · Paleoseismology · Seismic hazard · 2002 Çay earthquake

Extended author information available on the last page of the article

Published online: 21 May 2026

1 Introduction

The Anatolian plate of Türkiye is undergoing active westward tectonic escape driven by the northward convergence of the Arabian plate, with deformation primarily accommodated along the North Anatolian Fault Zone (NAFZ) and the East Anatolian Fault System (EAFS) (Fig. 1; McKenzie 1972; Dewey and Şengör 1979; Şengör 1979; Şengör et al. 1985). This tectonic framework produces a highly active deformation regime across the region. However, despite well-established plate-scale kinematics, the long-term earthquake behavior of individual fault segments remains poorly constrained, particularly in structurally complex transition zones.

The study area is located within the transition between the Central Anatolian Ova Province (CAOP) and the Western Anatolian Extensional Province (WAEP), where deformation is dominated by normal faulting. Such transition zones are characterized by complex fault geometries and variable earthquake recurrence behavior, making them critical targets for seismic hazard assessment. Although recent large earthquakes across Anatolia highlight the widespread occurrence of surface rupture, they provide limited constraints on long-term recurrence patterns. Therefore, constraining the Holocene earthquake history of individual fault segments, such as the Çay segment of the Sultandağı Fault, is essential for developing reliable seismic hazard models.

Recent large earthquakes emphasize the ongoing seismic hazard across Anatolia. These include the 6 February 2023 Kahramanmaraş earthquake doublet (Mw 7.7 and Mw 7.6) along the EAFS (e.g., Karabacak et al. 2023; Aksoy et al. 2023; Softa et al. 2024; Akgün and Softa 2025; Akgün et al. 2026); the Mw 6.1 Sındırgı earthquake pair (2025) in western

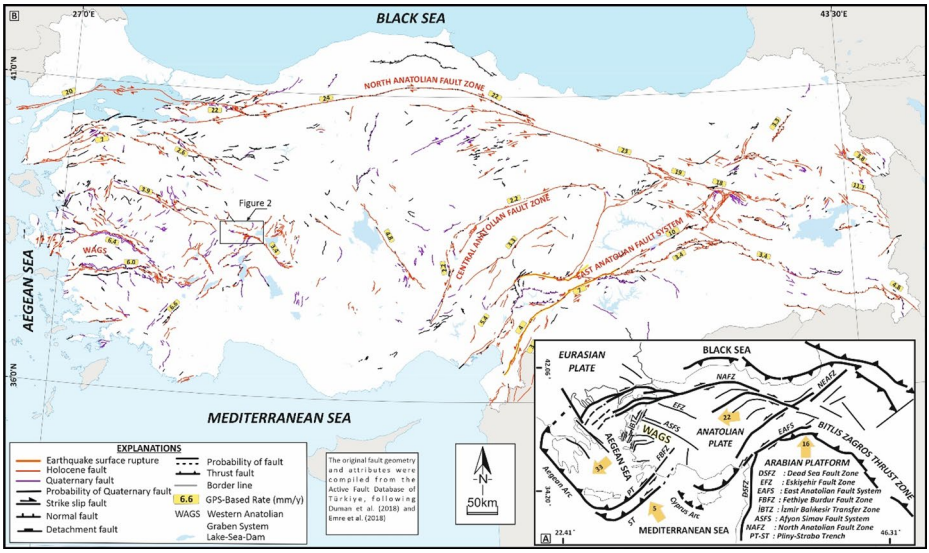

Fig. 1 **A** Regional tectonic setting of Anatolia, emphasizing the Western Anatolian Graben System (WAGS) (Gürer et al. 2004; Uzel et al. 2015). Yellow arrows show current plate-motion vectors, and accompanying values represent relative velocities (mm/yr) (Reilinger et al. 2006). **B** Seismotectonic map of Türkiye (adapted from [Emre et al. 2018; Duman et al. 2018]) displaying the spatial distribution of instrumental seismicity and major active fault zones that delineate the contemporary deformation regime of Anatolia

Anatolia (Kutoğlu et al. 2026a), the Mw 6.9 Samos earthquake (2020) in the Aegean extensional domain (e.g., Aktuğ et al. 2021), the Mw 6.8 Sivrice (Elazığ) earthquake (2020) on the EAFS (e.g., Güvercin et al. 2022; Akgün et al. 2025), and Mw 6.3 earthquakes along the Marmara region (e.g., Ertuncay et al. 2025). These events highlight the widespread occurrence of surface-rupturing earthquakes, yet they also underline the limited constraints on long-term recurrence behavior for individual fault segments such as the Çay segment.

Following major earthquakes, numerous studies have documented surface rupture geometry using GIS-based mapping and field observations (e.g., Softa 2024a). Detailed paleoseismological trenching remains essential to reconstruct long-term rupture histories and constrain earthquake recurrence. In western Anatolia, the most recent surface-rupturing earthquake affecting the study area is the Mw 6.5 Sultandağı event of 3 February 2002. The fault segment investigated here lies east of Afyonkarahisar (Fig. 1), within one of the most seismically hazardous regions of southwestern Türkiye. The earthquake occurred ~ 45 km southeast of Afyonkarahisar, causing 46 fatalities, 318 injuries, and moderate to heavy damage to 622 buildings (Emre et al. 2003). Rupture of the Sultandağı Fault near the apex of the Isparta Angle (Blumenthal 1963) produced a ~ 26-km-long surface rupture, with vertical displacements up to 21 cm and lateral offsets up to 15 cm (Emre et al. 2003; Figs. 1 and 2), demonstrating the fault's capacity for surface-breaking earthquakes and emphasizing its significance for regional seismic hazard.

Despite the high level of regional seismicity in Türkiye, no earthquakes of Mw ≥ 6.5, have occurred in western Anatolia following the 6 February 2023 earthquake doublet on the EAFS. This absence of recent large earthquakes, however, cannot be taken as evidence of seismic quiescence, given the short duration of instrumental records relative to recurrence

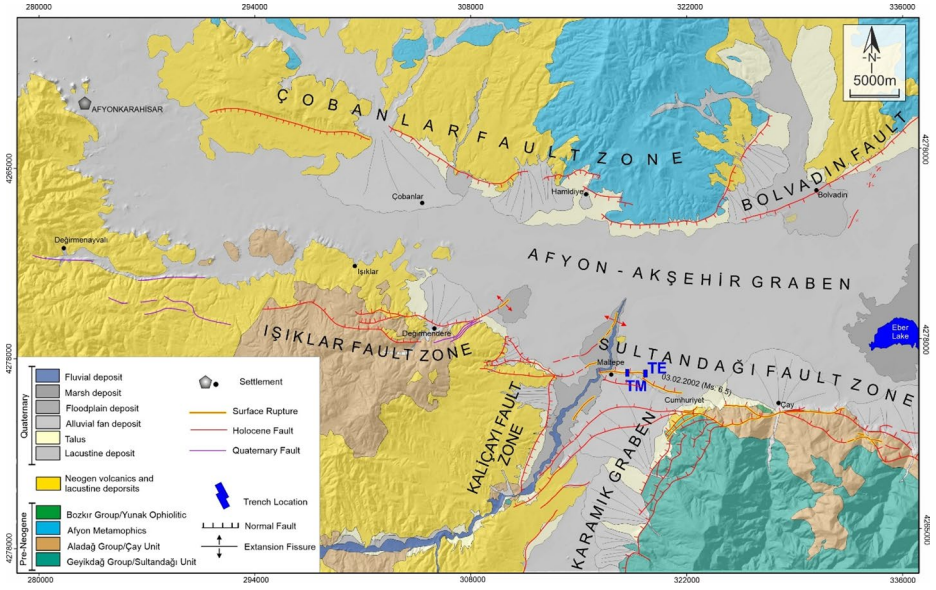

Fig. 2 Shaded-relief topographic map of the study area illustrating mapped active faults (compiled from Emre et al. 2018) together with the geological framework of the Afyon-Akşehir Graben and its surroundings, based on 1:100,000-scale geological maps of Öcal et al. (2011a, b)

intervals of surface-rupturing events. Therefore, constraining the Holocene earthquake history of the Çay segment is critical for reliable seismic hazard assessment.

In this study, we present new paleoseismological results from two trenches excavated across the 2002 surface rupture of the Sultandağı Fault. Trench stratigraphy, structural relationships, and radiocarbon (^{14}C) dating of faulted and unfaulted units are used to identify prehistoric surface-rupturing earthquakes, constrain their timing, and estimate recurrence intervals during the late Quaternary. Previous paleoseismological investigations along the Sultandağı Fault by Akyüz et al. (2006) established an initial framework; however, limited exposure and weak chronological control—particularly the absence of high-precision dating and quantitative uncertainty assessment—restricted the robustness of their results. In contrast, studies along the neighboring Simav Fault Zone document multiple Late Quaternary surface-rupturing events (Duman et al. 2013; Gürboğa 2013; Elmacı and Kürçer 2025), highlighting the critical role of high-resolution stratigraphic and chronological data in resolving earthquake recurrence within the Afyon–Akşehir–Simav extensional system.

The objectives of this study are to (i) identify the number of late Quaternary surface-rupturing paleoearthquakes on the Sultandağı Fault, (ii) constrain the timing and recurrence intervals of these events using radiocarbon dating, (iii) compare paleoseismic results with historical and instrumental seismicity in Western Türkiye, and (iv) evaluate implications for seismic hazard in the transition zone between the CAOP and WAEP. To achieve these objectives, two paleoseismological trenches were excavated across the Sultandağı Fault. Detailed trench logging was conducted, and fourteen samples were collected from key stratigraphic horizons to constrain the timing of past surface-rupturing events. Event ages were determined using radiocarbon (^{14}C) dating of faulted and unfaulted units, providing chronological control on late Quaternary faulting. The resulting chronology is further evaluated using Bayesian modeling and sensitivity analyses to ensure robustness against potential outliers.

2 Geological and tectonic settings

2.1 Tectonic framework and kinematic context

The Akşehir–Simav Fault System (ASFS) is an active extensional structure developed between the northeastern flank of the Isparta Angle and the southern margin of Central Anatolia (Koçyiğit and Özacar 2003). The graben system extends from Ilgın to the west of Afyonkarahisar and consists of multiple interacting normal faults with variable geometries and kinematics (Atalay 1975; Koçyiğit, 1984; Koçyiğit and Özacar 2003; Koçyiğit 2005; Bozkurt and Rojay 2005; Emre and Sözbilir, 2007). Within this system, the Sultandağı Fault forms one of the principal structures, extending for ~115 km with a general trend between N29E and N60W and comprising several geometrically distinct segments (Emre et al. 2018). The Çay Segment, located at the western termination of the fault system, is ~11 km long, dips northward, and ruptured during the 3 February 2002 earthquake sequence (Mw 6.5 and Mw 6.0), producing well-documented surface deformation (Özden et al. 2002; Demirtaş et al. 2002; Emre et al. 2003, 2018).

Despite this relatively well-defined structural framework, the kinematic evolution of the Sultandağı Fault remains debated. Early studies interpreted the structure as a reverse fault (e.g., Boray et al. 1985; Şengör et al. 1985; Şaroğlu et al. 1987, 1992; Barka et al. 1995),

whereas subsequent work redefined it as a normal fault within an extensional regime (e.g., Koçyiğit, 1984; Koçyiğit et al. 2000; Koçyiğit and Özacar 2003; Kutoğlu et al. 2026b). This discrepancy reflects fundamentally different models of regional neotectonic evolution and has direct implications for seismic hazard assessment. However, previous studies have largely presented these interpretations descriptively, without systematically testing them against stratigraphic or paleoseismological evidence. More importantly, although the 2002 surface rupture confirms the activity of the Çay Segment, the long-term behavior of the fault—including the correlation of paleoearthquakes between segments, the variability of recurrence intervals, and the degree of segment interaction—remains insufficiently constrained in the current literature.

2.2 Stratigraphy, basin evolution, and paleoseismological constraints

The northern boundary of the ASFS is defined by the Çobanlar and Bolvadin faults, both of which are normal faults with NW- and NE-trending orientations, respectively (Fig. 2). The southern margin of the graben is characterized by pre-Neogene basement rocks belonging to the Tauride orogenic belt (Özgül et al. 1991), whereas the northern margin is dominated by metamorphic rocks of the Afyon Zone (Öcal et al. 2011a, b). These basement units were tectonically overlain by the Yunak ophiolites during the Late Paleocene (Özgül 1976; Yeniyol 1979). These units are overlain by Neogene basin deposits, including limnic, fluvial, and volcanic sequences, which are in turn unconformably covered by Pliocene–Quaternary sediments. Quaternary deposits within the graben comprise lacustrine, alluvial fan, fluvial, and marsh environments, forming the primary archive for paleoseismological investigations. These unconsolidated deposits provide favorable conditions for preserving surface rupture and coseismic deformation associated with late Quaternary earthquakes. However, their depositional variability and lateral heterogeneity introduce uncertainties in stratigraphic interpretation and event identification. Such complexities place inherent limits on the resolution and completeness of trench-based paleoseismic records, particularly in extensional basin settings like the ASFS.

Although these limitations have been recognized, they have not been systematically evaluated in previous studies of the Sultandağı Fault. In this context, the present study moves beyond a descriptive geological framework by addressing how these stratigraphic and tectonic factors influence the reliability of paleoseismological interpretations. By integrating trench stratigraphy with radiocarbon dating and Bayesian modeling, the study aims to provide a more robust and quantitatively constrained reconstruction of earthquake history, directly addressing the unresolved issues identified above.

3 Methodology

Two paleoseismological trenches, Maltepe and Eskiköprü, were excavated across the surface rupture produced by the 3 February 2002 Mw 6.5 Çay earthquake on the Çay Segment of the Sultandağı Fault (Figs. 1 and 2). Trench sites were selected directly on the well-preserved coseismic rupture, which had been mapped in detail shortly after the earthquake using field observations and geospatial analyses (Emre et al. 2011). The availability of pre-

cise surface rupture data enabled accurate trench placement across the main fault trace and minimized uncertainty related to fault geometry.

Trenches were excavated perpendicular to the fault strike to expose fault-zone stratigraphy and deformation structures associated with repeated surface-rupturing earthquakes. Paleoseismological investigations followed standard procedures outlined by McCalpin (2009), including systematic cleaning, smoothing, and stabilization of trench walls to enhance the visibility of sedimentary units and structural features. Each trench wall was gridded using a 1 × 1 m reference framework to ensure spatial control during logging, sampling, and interpretation.

High-resolution photographic documentation was conducted for all trench walls. Multiple overlapping photographs (minimum ~ 30% overlap) were acquired under consistent lighting conditions. Photomosaics were generated using a GIS-based workflow in ArcGIS, adhering to methodologies similar to those described by Kürçer et al. (2016); Softa (2024b); Öncü et al. (2024), and Şengöçmen Geçkin et al. (2022). Grid intersection points were used as control nodes to georeference individual images, which were subsequently merged into composite photomosaics. These mosaics provided a high-resolution base for detailed stratigraphic and structural logging.

Trench logging focused on identifying sedimentary units, fault strands, colluvial wedges, fissure fills, growth strata, and other deformation features indicative of past surface faulting. Paleoearthquake events were interpreted based on stratigraphic relationships, upward fault terminations, and event-related depositional units, following established paleoseismological criteria.

Fourteen radiocarbon samples were collected from stratigraphic horizons bracketing individual surface-faulting events. Sampling focused on well-defined units immediately above and below event horizons, following established trench paleoseismology protocols to minimize reworking, inheritance, and contamination effects.

To ensure stratigraphic reliability, paired samples were obtained from both faulted and unfaulted correlatives, including displaced units across the fault zone. These were evaluated within a Bayesian chronological framework to test internal consistency between stratigraphy and age estimates.

The sampled materials include charcoal, bone, and bulk organic-rich sediments. Particular emphasis was placed on charcoal, with an increased number of samples ($n = 14$) to strengthen chronological control. Charcoal fragments were carefully selected based on angular morphology and preservation within primary depositional matrices, and reworked or abraded material was excluded. The additional charcoal sample yielded an $F^{14}C$ signature consistent with modern or recent carbon input, providing an independent validation of near-surface depositional ages and confirming the absence of significant reworking in younger units.

Bone samples were assessed in terms of preservation state and depositional context to distinguish in situ material from potential reworking; no sedimentological or taphonomic evidence for transport was observed. Bulk sediment samples were limited to fine-grained, low-energy depositional environments (e.g., overbank or lacustrine settings) lacking erosional contacts or signs of mixing.

To evaluate potential old-carbon or inheritance effects, bulk sediment ages were systematically compared with charcoal and bone ages from equivalent or stratigraphically bounding levels. All radiocarbon ages are stratigraphically consistent, with no age inver-

sions observed within 95.4% probability ranges. This agreement demonstrates that the dated materials are reliable and that the resulting chronology is robust, with ages fully compatible with their respective stratigraphic positions and depth relationships.

In addition, sensitivity analyses were conducted within the Bayesian modelling framework in OxCal, following the outlier detection approach of Bronk Ramsey (2009). A Student's t-type outlier model was applied to all radiocarbon determinations to identify and downweight potential anomalous ages. Model performance was assessed using agreement indices and convergence parameters, all of which fall within acceptable ranges. The results indicate that no individual age determination disproportionately influences the model, and that the overall chronology remains stable under varying assumptions. All samples were dated using AMS radiocarbon methods at TÜBİTAK MAM and calibrated in OxCal (Bronk Ramsey 2009) with the IntCal20 curve. A Bayesian Sequence model incorporating stratigraphic ordering constraints was used to calculate posterior age distributions and inter-event times at the 95.4% confidence level (2σ). This approach integrates laboratory uncertainty with depositional superposition principles and provides a statistically robust chronological framework for Holocene surface-rupturing events along the Çay Segment.

This integrated methodology-combining precise trench placement, standardized paleoseismological logging, GIS-based photomosaic construction, and IntCal20-calibrated radiocarbon dating-provides a robust framework for reconstructing the paleoseismic history and assessing the seismic hazard potential of the Sultandağı Fault.

4 Results

4.1 Paleoseismological investigation

4.1.1 Maltepe trench

The Maltepe trench site is located approximately 10 km west of Çay town, near Maltepe village (Fig. 3), on Quaternary deposits affected by the surface rupture of the 2002 Çay earthquake. The trench was excavated perpendicular to the fault trace with a strike of N10W and dimensions of ~12 m length, 4 m width, and up to 2.5 m depth. A~6 m–wide deformation zone disturbing Holocene sediments is exposed within the trench. The main fault observed in the trench strikes N70E and dips steeply, displaying predominantly normal-slip kinematics consistent with the regional geometry and tectonic character of the Sultandağı Fault.

Seven stratigraphic units were identified in the trench wall (Fig. 4). Selected units were radiocarbon dated at the TÜBİTAK Marmara Research Center (Table 1), providing chronological constraints on surface-rupturing paleoearthquakes. The lowermost exposed unit (Unit 1) consists of greenish-gray, laminated clayey mud that is laterally continuous and subhorizontal (Fig. 4). This unit is displaced by a normal fault, defining the oldest recognized paleoearthquake (Event E1). Unit 1 is slightly eroded and unconformably overlain by Unit 2, indicating post-event surface modification prior to renewed sedimentation.

Unit 2 is composed of whitish-gray clayey silt with scattered cobbles (Fig. 4). A charcoal-rich horizon within this unit yielded a radiocarbon age of 1190±25 year BP (Table 1). Unit 3 conformably overlies Unit 2 and consists of blackish-gray, organic-rich mud with abundant organic fragments. This unit is laterally continuous, with a maximum thickness of



Fig. 3 **A** Oblique satellite view of the study area highlighting the Çay Segment of the Sultandağı Fault, the examined surface scarp, and the trench site. **B** Surface rupture associated with the 3 February 2002 Çay earthquake (photo courtesy of Selim Özalp, taken shortly after the event); arrows indicate the main rupture strands. View to the east. **C** Ground photograph of the trench excavation along the mapped surface rupture trace. View to the south

~15–20 cm. Bone samples collected from Unit 3 yielded radiocarbon ages of 1141 ± 26 year BP.

Unit 4 overlies Unit 3 and is characterized by yellowish-beige silty mud. No direct radiocarbon age is available for Unit 4. The overlying Unit 5 consists of beige, granule-rich mud with a distinct erosional basal contact (Fig. 4). A radiocarbon sample from Unit 5 yielded an age of 1092 ± 23 year BP, providing a maximum age constraint for deformation affecting Unit 4. Unit 6 is represented by brownish-beige, granule-rich mud and is overlain by SF-ÇS-MAL1-D-C5 was obtained from Unit 7, a ~ 35 cm thick modern soil layer that is clearly cut by the surface rupture associated with the 2002 earthquake. The sample is reported as $F^{14}C$, indicating a post-bomb origin, and calibrates to 1958–1990 CE. This result is consistent with the modern depositional age of Unit 7 and supports its interpretation as the most recent pre-earthquake soil horizon.

Trench observations at the Maltepe site reveal evidence for three surface-rupturing seismic events. The earliest event (E1) is defined by faulting of Unit 1 and burial by Unit 2, constraining its occurrence to prior to the deposition of Unit 2. Due to the lack of abso-

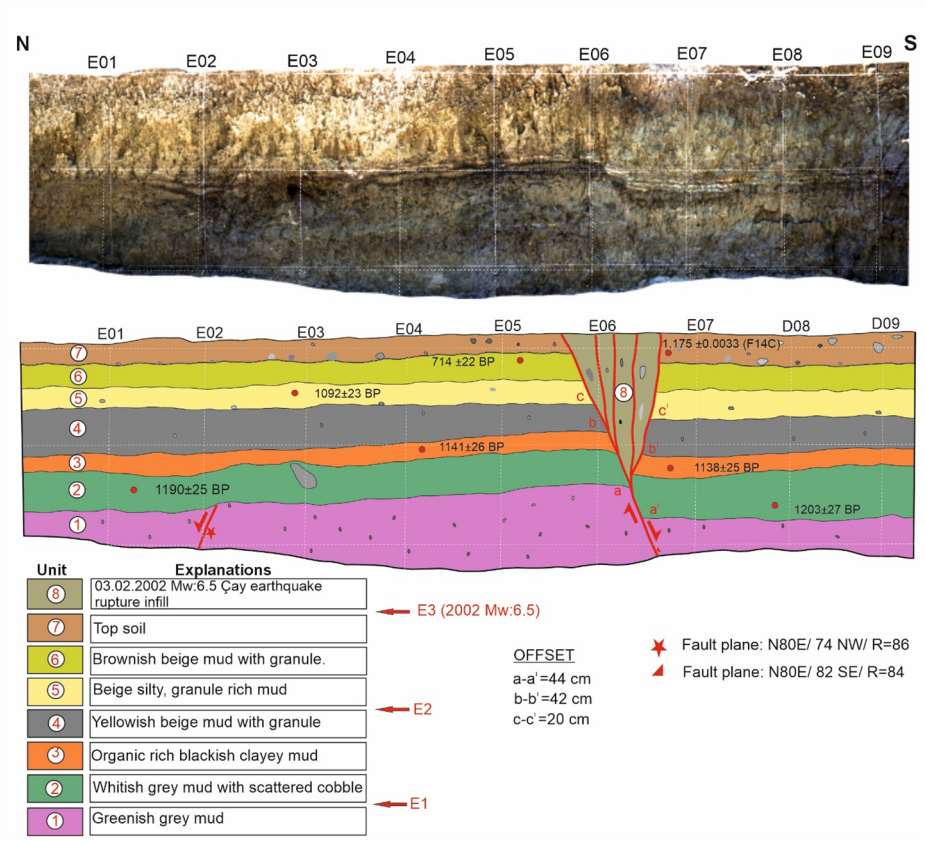

Fig. 4 Photomosaic of the east wall of the Maltepe trench and its corresponding paleoseismological log

Table 1 Radiocarbon ages obtained from charcoal and bone samples collected from stratigraphic units exposed in the Maltepe trench excavations

Sample Nr	Lab. code	Unit	Dated material	Conventional age (BP)
SF-ÇS-MAL1-D-C1	1729	Unit 3	Bone	1138±25
SF-ÇS-MAL1-D-C2	1730	Unit 3	Bone	1141±26
SF-ÇS-MAL1-D-C3	1731	Unit 2	Charcoal	1190±25
SF-ÇS-MAL1-D-C4	1732	Unit 2	Charcoal	1203±27
SF-ÇS-MAL1-D-C5	1733	Unit 7	Charcoal	1.175±0.0033*
SF-ÇS-MAL1-D-C6	1734	Unit 5	Bulk sediment	1092±23
SF-ÇS-MAL1-D-C7	1735	Unit 6	Bulk sediment	714±22

*SF-ÇS-MAL1-D-C5 is reported as $F^{14}C$ rather than a conventional calibrated BP age because it represents a post-bomb sample. The measured $F^{14}C$ value reflects elevated atmospheric radiocarbon levels associated with nuclear testing and therefore provides more appropriate chronological information than a conventional age. Calibration using the NH2 post-bomb atmospheric curve indicates that the sample dates between 1958 and 1990 CE (Hua et al. 2022; Reimer et al. 2020)

lute age control on Unit 1, the timing of E1 remains poorly constrained but must predate 1190 ± 25 year BP. The penultimate event (E2) is inferred from differences in vertical separation between Units 4 and 5, expressed by offsets aa', bb', and cc' along the fault plane (Fig. 4). This event postdates deposition of Unit 4 and predates accumulation of Unit 5. Radiocarbon ages from Unit 3 (1141 ± 26 year BP) and Unit 5 (1092 ± 23 year BP) constrain Event E2 to have occurred between ~ 1140 and ~ 1090 year BP. The most recent event (E3) postdates the deposition of Unit 4 and is younger than 714 ± 22 year BP, based on stratigraphic relationships and the preservation of near-surface deformation. This event corresponds to the 2002 Çay earthquake, which produced surface rupture cutting the modern soil (Unit 7) and generated an additional ~ 20 cm of vertical displacement. Following Event E2, the top of Unit 4 in the hanging wall was partially eroded, and cumulative displacement was increased during the 2002 rupture.

4.1.2 Eskiköprü trench

The Eskiköprü trench is located approximately 1.5 km east of Maltepe village, along the clearly traceable surface rupture of the most recent earthquake (Fig. 5). The trench was excavated perpendicular to the fault trace and measures ~ 15 m in length, 4 m in width, and 3 m in depth. A 1.5–2 m–wide deformation zone affecting Holocene deposits is exposed in the trench wall. The fault strikes ~ 070° and displays predominantly normal-slip kinematics.

Fourteen stratigraphic units were distinguished (Fig. 6; Table 2). The lowermost exposed Unit 1 consists of fine- to medium-pebble gravel interbedded with organic-rich blackish-gray mud. Unit 2 is composed of black muddy and silty marsh deposits and is overlain by Unit 3, represented by organic-rich blackish-brown mud. Unit 4 overlies Unit 3 with an erosional contact and consists of beige silty mud. A radiocarbon sample from Unit 4 yielded an age of 6224 ± 38 year BP (Table 2). Unit 5 is subdivided into Units 5a and 5b. Unit 5a consists of light beige sandy mud and yielded a bulk radiocarbon age of 5699 ± 38 year BP. Unit 5b comprises dark beige silt and fine sand and was dated to 4879 ± 31 year BP. Unit 6 consists of light beige, granule-rich mud and fine sand with an erosional basal contact. This unit yielded a radiocarbon age of 4392 ± 29 year BP. Unit 7 is composed of light brown mud with fine sand lenses and was dated to 3738 ± 31 year BP. Unit 8, which overlies Unit 7 with an erosional contact, consists of gray granule-rich sand and yielded an age of 3386 ± 27 year BP. Unit 9 erosionally overlies Unit 8 and is 35–40 cm thick, characterized by light beige clay and fine sand. Unit 10 overlies Unit 9 with an erosional base and consists of gray fine- to medium-grained sand. Unit 11 is composed of light brown muddy fine sand. Unit 12 overlies Unit 11 with an erosional contact and consists mainly of beige silty clayey mud; a bulk sample from this unit yielded an age of 3123 ± 26 year BP. Unit 13 represents modern soil and is displaced by the most recent earthquake. Unit 14 consists of rupture-fill sediment formed along the fault plane.

Three surface-rupturing earthquakes are identified in the Eskiköprü trench. Event E1 is defined by faulting of Unit 5b, which records ~ 23 cm of vertical displacement (Fig. 5). The event horizon corresponds to the contact between Units 5b and 6. Unit 5b is cut by the fault, whereas Unit 6 drapes and seals the rupture. Radiocarbon ages from Unit 5b (4879 ± 31 year BP) and Unit 6 (4392 ± 29 year BP) constrain Event E1 to between ~ 4880 and ~ 4390 year BP. Event E2 is identified at the contact between Units 7 and 8. The fault cuts Unit 7 and is overlain by Unit 8, indicating burial of the rupture (Fig. 6). Radiocarbon ages from Unit 7



Fig. 5 **A** Oblique satellite view of the study area highlighting the Çay Segment of the Sultandağı Fault, the examined surface scarp, and the trench site. **B**, **C** Surface rupture associated with the 3 February 2002 Çay earthquake (photo courtesy of Selim Özalp, taken shortly after the event); arrows indicate the main rupture strands. View to the east

(3738 ± 31 year BP) and Unit 8 (3386 ± 27 year BP) constrain Event E2 to between ~3740 and ~3390 year BP. Event E3 corresponds to the 2002 earthquake (Mw 6.5), which produced ~25 cm of vertical displacement, including offset of the modern soil (Unit 13). Rupture-fill deposits (Unit 14) formed along the fault trace during this event.

4.2 Radiocarbon-based bayesian sensitivity analysis and model robustness

Sensitivity analyses were performed to evaluate the robustness of the modeled earthquake chronology under different assumptions and data-selection strategies. This approach is particularly important in paleoseismology, where sediment-derived radiocarbon samples may be affected by reworking or incorporation of inherited carbon. By testing the influence of individual samples within a Bayesian framework, it is possible to assess whether the inferred event ages remain stable despite such uncertainties following the Bronk Ramsey (2009) and Scharer et al. (2024). The model was defined as a stratigraphically constrained sequence composed of two depositional phases bounded by three surface-faulting events (E1-E3) identified in both trenches.

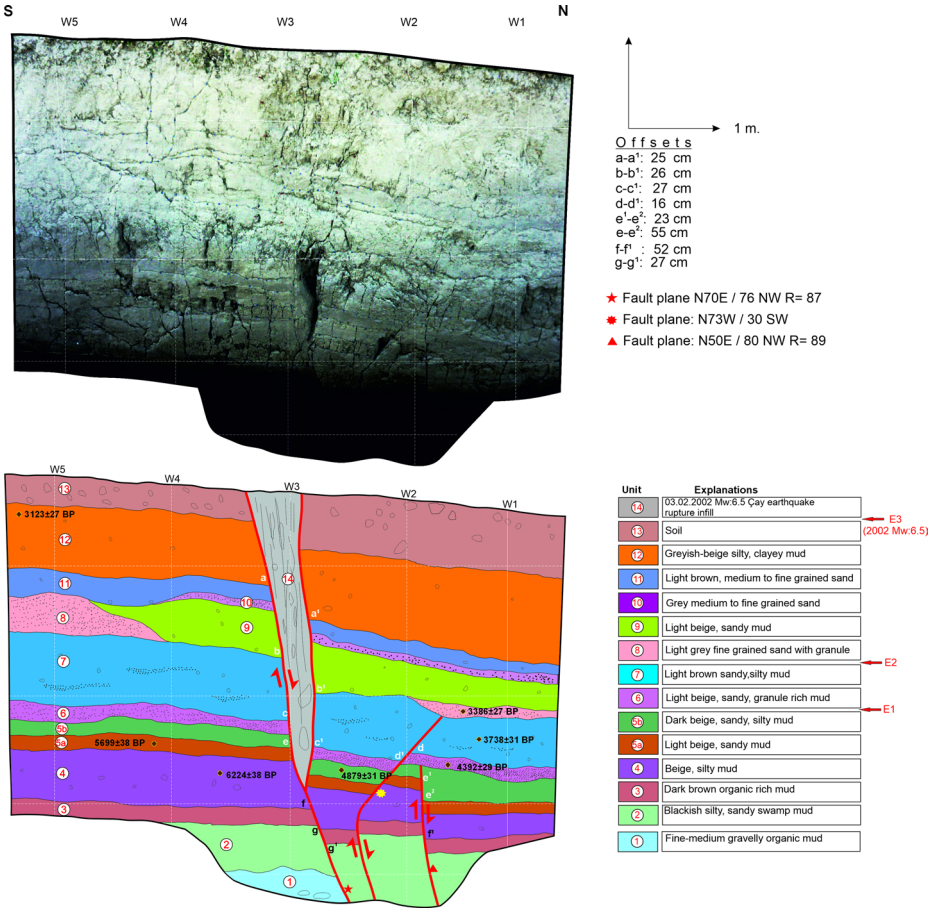

Fig. 6 Photomosaic of the east wall of the Eskiköprü trench and its corresponding paleoseismological log

Table 2 Radiocarbon ages obtained from bulk sediment collected from stratigraphic units exposed in the Eskiköprü trench excavations

Sample Nr.	Lab. Code	Unit	Dated material	Conventional age (BP)
SF-EKH-B-C1	1738	Unit 4	Bulk sediment	6224±38
SF-EKH-B-C2	1739	Unit 6	Bulk sediment	4392±29
SF-EKH-B-C3	1740	Unit 8	Bulk sediment	3386±27
SF-EKH-B-C4	1741	Unit 12	Bulk sediment	3123±26
SF-EKH-B-C5	1742	Unit 5b	Bulk sediment	4879±31
SF-EKH-B-C6	1743	Unit 5a	Bulk sediment	5699±38
SF-EKH-B-C7	1744	Unit 7	Bulk sediment	3738±31

In the Maltepe trench, the lower phase includes samples SF-ÇS-MAL1-D-C1 to C4, representing deposition between events E1 and E2, while the upper phase comprises samples SF-ÇS-MAL1-D-C6 and C7, corresponding to deposition between E2 and E3 (Fig. 7).

In the Eskiköy trench, the lower phase includes samples SF-EKH-B-C1, C5, and C6 (pre-E1), whereas samples SF-EKH-B-C2 and C7 represent deposition between E1 and E2. The upper phase consists of samples SF-EKH-B-C3 and C4, deposited between E2 and E3. In both trenches, the youngest boundary (E3) is independently constrained by the historically documented 2002 Çay earthquake (Fig. 8).

Model diagnostics demonstrate excellent statistical performance. All dated samples and modeled boundaries show high convergence values (~100), indicating stable Markov Chain Monte Carlo sampling and strong agreement between the stratigraphic framework and the radiocarbon likelihoods. To further assess the influence of potentially anomalous samples, an outlier analysis following the approach of Bronk Ramsey (2009) was implemented using a Student's t-type model. This approach allows individual radiocarbon determinations to deviate from the model and quantifies the probability of outlier behavior. The outlier model parameters show high convergence (T(5): C=95; U(0,4): C~100), indicating stable parameter estimation. Importantly, none of the samples were significantly down-weighted, and all determinations retained high agreement and convergence values (~100), (Fig. 9).

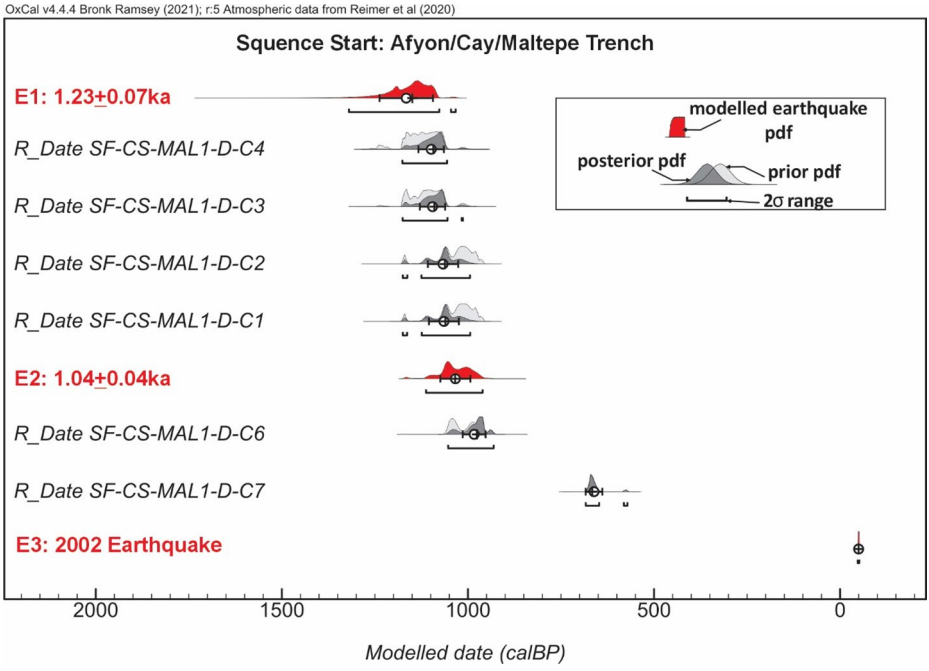

Fig. 7 Bayesian chronological model for the Maltepe trench (Çay segment, Sultandağı Fault) constructed in OxCal v4.4.4 (Bronk Ramsey 2008, 2009; IntCal20; Reimer et al. 2020). Stratigraphically constrained sequence with two depositional phases bounded by three surface-faulting events (E1–E3). Student's t-type outlier model (Bronk Ramsey 2009) confirms internal consistency (posterior outlier probabilities~0). Convergence values (~100) indicate stable model performance. The 2002 Çay earthquake provides independent historical constraint for E3. Sensitivity analysis (removal of youngest sample from each phase) yields negligible age shifts (≤±2 years)

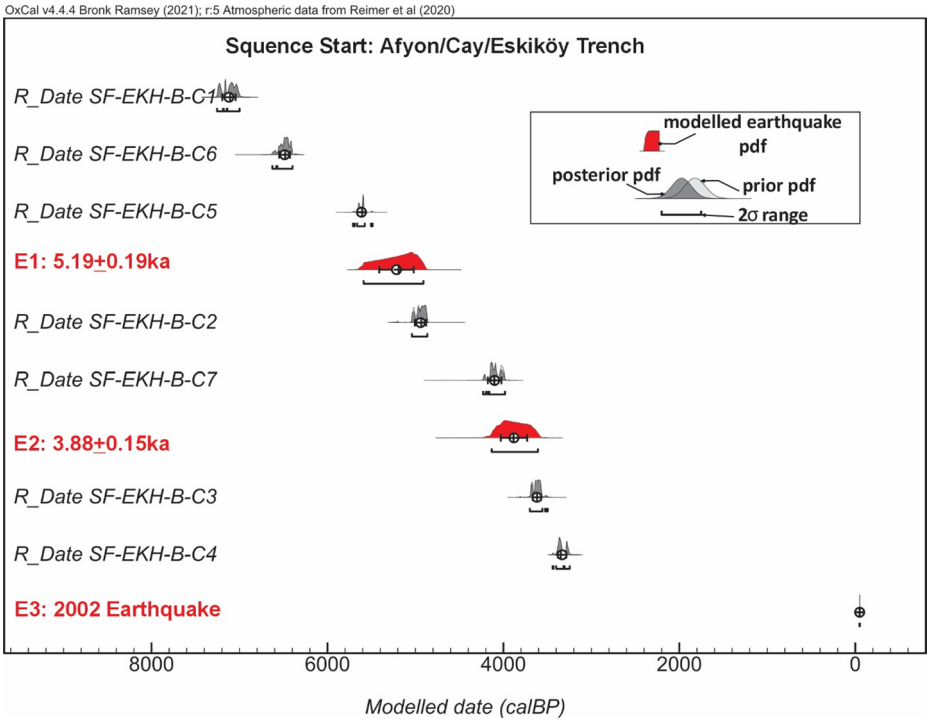

Fig. 8 Bayesian chronological model for the Eskiköy trench (Çay segment, Sultandağı Fault) constructed in OxCal v4.4.4 (Bronk Ramsey 2008, 2009; IntCal20; Reimer et al. 2020). Stratigraphically constrained sequence with three depositional phases bounded by three surface-faulting events (E1–E3). Student's t-type outlier model (Bronk Ramsey 2009) confirms internal consistency (posterior outlier probabilities ~ 0). Convergence values (~ 100) indicate stable model performance. The 2002 Çay earthquake provides independent historical constraint for E3. Sensitivity analysis (removal of youngest sample from each phase) yields maximum age variation of ± 7 years

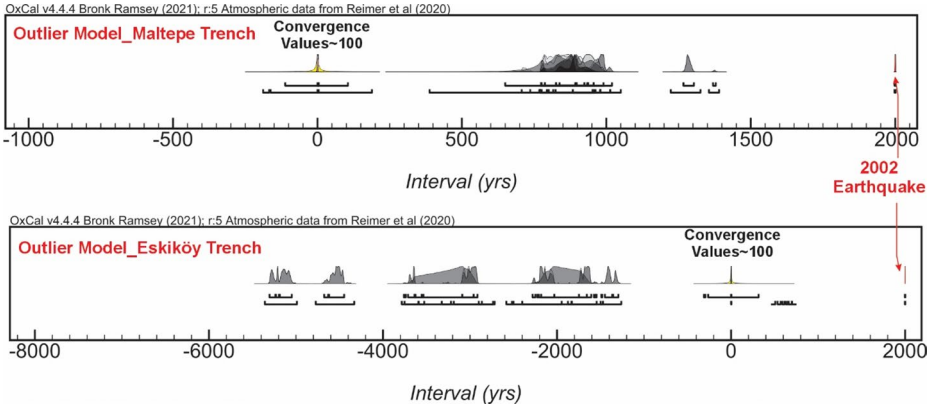

Fig. 9 Outlier analysis for the Maltepe and Eskiköy trenches (OxCal v4.4.4; IntCal20). All samples show posterior outlier probabilities approaching zero and convergence values ~ 100, indicating no statistically significant outliers. The Student's t-type outlier model (Bronk Ramsey 2009) confirms internal consistency of both radiocarbon datasets and supports the robustness of the event chronology

Sensitivity of the model to potential reworking effects was further assessed by removing the youngest radiocarbon sample from each stratigraphic phase and rerunning the Bayesian analysis. In the Maltepe trench, mean posterior ages shifted by less than ±2 years for both events (E1: from 1231±72 BP to 1230±70 BP; E2: from 1040±40 BP to 1042±41 BP). In the Eskiköy trench, shifts were similarly minimal (E1: from 5191±196 BP to 5192±195 BP; E2: from 3884±150 BP to 3891±145 BP), with maximum variation of ±7 years. All variations are well within the 1σ uncertainty ranges of the preferred model, confirming that the modeled earthquake chronology is robust and insensitive to individual data points. No single radiocarbon determination exerts a disproportionate influence on the results. Furthermore, the independent historical constraint provided by the 2002 Çay earthquake effectively anchors the upper boundary of the model, enhancing chronological control for the youngest event. Overall, these results confirm that the derived event chronology is reliable and provides a robust temporal framework for interpreting surface-faulting history and assessing earthquake recurrence in the study area.

5 Discussion

5.1 Tectonic framework of the Akşehir-Simav Fault System

The Akşehir-Simav Fault System (ASFS) constitutes one of the principal extensional tectonic systems of western Anatolia, accommodating regional N-S crustal extension through a set of high-angle normal faults (e.g., Koçyigit et al. 2000; Koçyigit and Deveci, 2007; Ozkaymak et al. 2019; Tiryakioglu et al. 2018; Solak et al. 2026). The Sultandağı Fault forms the central structural component of this system, and the Çay segment represents one of its most morphologically and seismically active sections (e.g., Emre et al. 2003, 2018). Geomorphological investigations along the Sultandağı Fault within the ASFS document well-preserved fault scarps, triangular facets, hanging-wall basin development, and youthful mountain-front morphologies, all indicative of sustained Quaternary deformation (e.g.Topal et al. 2016; Özkaymak et al. 2019; Topal and Softa 2023; Kutoğlu et al. 2026a). These morphometric indicators collectively point to ongoing tectonic activity and repeated surface-rupturing earthquakes during the late Quaternary. This interpretation is consistent with the broader neotectonic framework of Türkiye, a region characterized by high seismicity and frequent moderate-to-large earthquakes (Topal et al. 2016; Softa 2022; Akgün 2024; Akgün et al. 2025; Kutoğlu et al. 2026a). The regional significance of the AASS has been highlighted by instrumental and historical seismicity. The 2002 Çay earthquake sequence (Mw 6.5 and Mw 6.0) produced a well-defined surface rupture along the Sultandağı Fault (Emre et al. 2003; Akyüz et al. 2006). More recently, the 2025 Sındırgı earthquake doublets (Mw 6.1) occurring along the westernmost sector of the Afyon-Simav Fault System (ASFS) further highlighted the seismic potential of this extensional fault network and the dynamic interaction between its constituent segments (Kutoğlu et al. 2026a). The occurrence of closely spaced doublets suggests stress redistribution within the system and underscores the role of segment-to-segment stress transfer in controlling rupture patterns.

In this context, the spatial progression of moderate-magnitude earthquakes along the ASFS raises the question of possible west-east (or along-strike) earthquake migration toward the Çay-Simav segment. Although deterministic forecasting is not warranted, Cou-

lomb stress interactions and historical rupture sequencing indicate that adjacent segments within an extensional regime may experience elevated failure probability following nearby moderate events. Therefore, the recent activity at Sındırgı reinforces the need to evaluate the Çay segment not as an isolated structure but as part of a mechanically coupled fault system with potential for cascading or time-clustered ruptures.

5.2 Chronological robustness and sensitivity of the Holocene earthquake chronology on the Çay segment-implications for slip rate and recurrence

The paleoseismological investigations at the Maltepe and Eskiköprü trenches provide a robust Holocene earthquake record for the Çay segment of the Sultandağı Fault. By integrating detailed stratigraphic observations, structural relationships, radiocarbon dating, and Bayesian chronological modeling, the temporal framework of past surface-faulting events is significantly refined. The Bayesian age modeling was performed using OxCal (Bronk Ramsey 1994, 1995, 2001), allowing the incorporation of stratigraphic ordering constraints together with analytical uncertainties associated with radiocarbon determinations.

A key aspect of this study is the implementation of sensitivity analyses to evaluate the robustness of the earthquake chronology. Such analyses are critical in paleoseismology, particularly when sediment-derived radiocarbon samples may be influenced by reworking or inherited carbon (e.g., Bronk Ramsey 2009; Scharer et al. 2024). In this study, sensitivity testing was conducted through three complementary approaches: (i) application of a Student's t-type outlier model, (ii) evaluation of model convergence behavior, and (iii) removal of the youngest radiocarbon sample from each stratigraphic phase to test for potential reworking effects. Unlike previous compilations that combined data from multiple studies with differing trench methodologies, this study restricts Bayesian analysis to trench data collected under a consistent field and dating protocol, thereby eliminating uncertainties associated with cross-site event correlation.

The outlier analysis demonstrates that posterior outlier probabilities approach zero, meaning that none of the samples behave as statistically significant outliers. All radiocarbon determinations exhibit very high convergence values (~100), indicating stable model performance and strong agreement between the data and the imposed stratigraphic framework. To further assess model robustness, the youngest radiocarbon sample from each stratigraphic phase was removed and the model was rerun. In the Maltepe trench, mean posterior ages shifted by less than ±2 years for both events; in the Eskiköprü trench, the maximum variation was ±7 years. All variations fall well within the 1σ uncertainty ranges of the preferred model, confirming that no single radiocarbon determination exerts a disproportionate influence on the modeled event ages and that the chronology is robust to potential reworking effects.

The reliability of the chronological model is further supported by the depth-dependent stratigraphic consistency of the radiocarbon ages. All dated samples are compatible with their respective stratigraphic positions and event-bounding relationships, with no age inversions observed. In particular, sample SF-ÇS-MAL1-D-C5, reported as $F^{14}C$, yields a post-bomb signature consistent with modern carbon and calibrates to the period 1958–1990 CE. This sample was obtained from Unit 7, the uppermost soil horizon, which is directly overlain and truncated by deposits associated with the 2002 earthquake. Its agreement with the

expected modern age provides an independent validation of the stratigraphic framework and confirms the absence of significant reworking in the youngest units.

All modeled event ages and inter-event times were evaluated at the 95.4% probability level (2σ), which represents the standard confidence interval widely used in probabilistic seismic hazard assessment (PSHA). The combined chronologies from the Maltepe and Eskiköprü trenches indicate a total of five Holocene surface-rupturing earthquakes, including the most recent 2002 event. The modeled event ages are E1: 5.19 ± 0.11 ka, E2: 3.86 ± 0.14 ka, E3: 1.65 ± 0.47 ka, E4: 0.84 ± 0.10 ka, and E5: 2002 CE. The corresponding inter-event times range from approximately 0.30 to 2.21 kyr, with uncertainties extending up to ~2.82 kyr (Table 3; Fig. 10). This variability suggests that the Çay segment does not exhibit strictly periodic recurrence. Instead, the late Holocene appears characterized by temporal clustering of events. The vertical offsets observed in the trenches (~20–25 cm per event) are consistent with field measurements from the 2002 rupture, indicating that moderate-magnitude (Mw ≥ 6) earthquakes represent the dominant seismic mode of the segment. Although stratigraphic offsets of up to 55 cm are observed in the trench walls, these are interpreted as cumulative pre-2002 displacements rather than single-event slip. The geometry and superposition of event horizons indicate progressive scarp growth through repeated surface ruptures. A comparable multi-event rupture pattern has been documented after the 2023 Kahramanmaraş earthquakes (Softa et al. 2024), where recent ruptures reactivated pre-existing scarps. Accordingly, the Çay Segment record reflects cumulative deformation from successive Holocene earthquakes rather than an isolated displacement event. Further, because the 95.4% intervals are already embedded in the Bayesian posterior outputs, the chronological model inherently satisfies the confidence requirements typically imposed in PSHA applications. The use of stratigraphically constrained Bayesian modeling therefore

Table 3 Earthquake timing, interevent time, and recurrence interval along the Çay segment

E[a]	Dates A (ka)			Interevent time I (ka) (AE_{first}–AE_{second})			Recurrences interval[b] R (ka)		
	A_{min}	$A_{average}$	A_{max}	I_{min} (AE_{min}–AE_{max})	$I_{average}$ ($AE_{average}$–$AE_{average}$)	I_{max} (AE_{max}–AE_{min})	R		
							R_{min}	$R_{average}$	R_{max}
E1	5.08	5.19	5.30				0.73	1.16	1.59
				1.08	1.33	1.58			
E2	3.72	3.86	4.00						
				1.60	2.21	2.82			
E3	1.18	1.65	2.12						
				0.24	0.81	1.38			
E4	0.74	0.84	0.94						
				0.01	0.30	0.59			
E5	0.35	0.54	0.73						

[a]According to the preferred model derived from Oxcal (Bronk Ramsey 2008, 2009; Reimer et al. 2009)

[b]Recurrence interval based on the formula (Duran et al. 2021)

The formula are as given below:

Rmin: ((AE1min − AE2max) + (AE2min – AE3max) + (AE3min – AE4max) + (AE4min – AE5max))/n − 1

Raverage: ((AE1average − AE2average) + (AE2average − AE3average) + (AE3average − AE4average) + (AE4average − AE5average))/n − 1

Rmax:((AE1max − AE2min) + (AE2max – AE3min) + (AE3ma x– AE4min) + (AE4max – AE5min))/n − 1

E, events; n, number of events

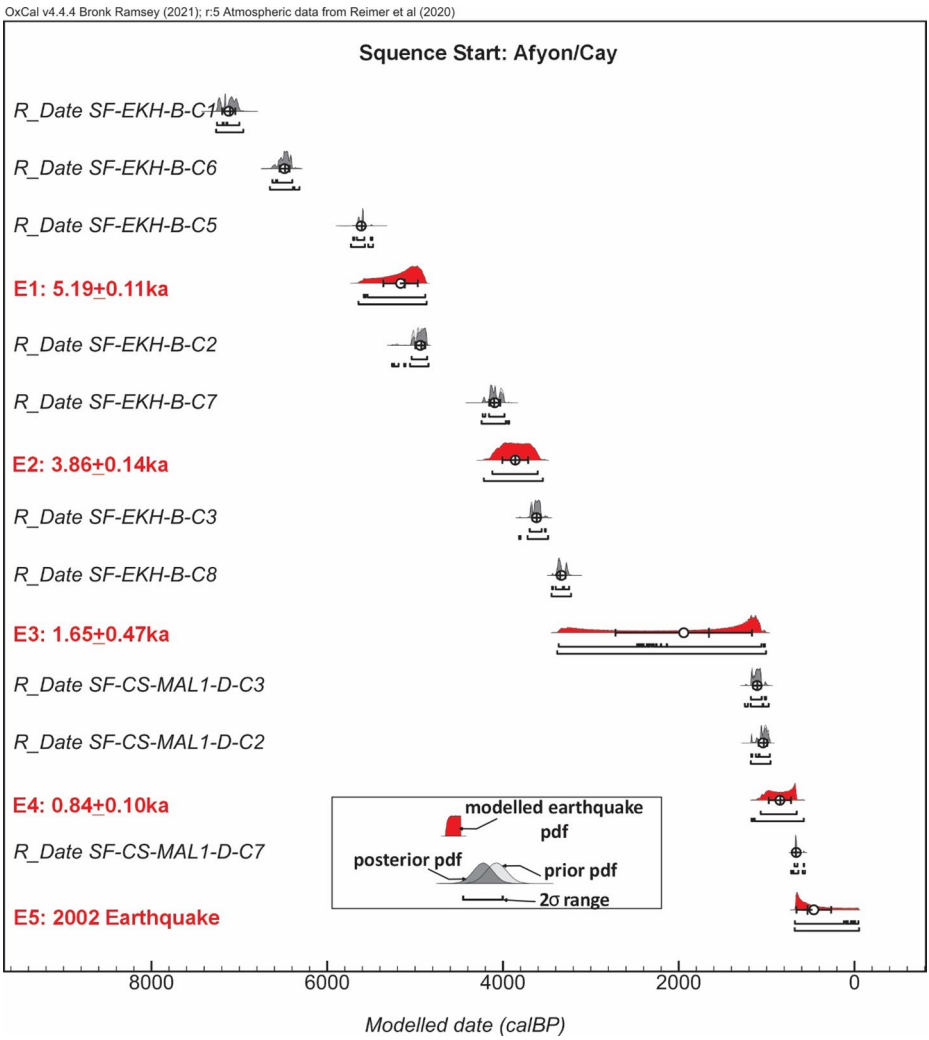

Fig. 10 The preferred Bayesian model (OxCal v4.4.4; IntCal20; Bronk Ramsey 2008, 2009; Reimer et al. 2020) constrains five Holocene surface-rupturing earthquakes (E1–E5) on the Çay segment. The stratigraphically constrained sequence integrates radiocarbon data from the Maltepe and Eskiköy trenches. The 2002 Çay earthquake (Mw 6.5) anchors the youngest event (E5)

represents a methodological strength of the study, reducing chronological ambiguity while preserving realistic epistemic uncertainty. Further, the sensitivity analyses demonstrate that these recurrence intervals are not controlled by individual radiocarbon ages but rather reflect a stable and coherent chronological framework. Overall, the agreement between stratigraphy, radiocarbon data, Bayesian modeling, and sensitivity analysis provides strong confidence in the reconstructed earthquake history. This robust chronological framework has direct implications for seismic hazard assessment, as it supports reliable estimates of earthquake recurrence and temporal clustering behavior along the Çay segment of the Sultandağı Fault.

Previous paleoseismological investigations along the Sultandağı Fault by Akyüz et al. (2006) represent the first effort to document surface-faulting history on the Çay segment following the 2002 earthquake. Their study, based on trenching at Maltepe and Çay, analyzed six radiocarbon samples (mainly described charcoal) using conventional Libby decay counting at the Poznań laboratory. Two samples were identified as stratigraphically inconsistent, indicating potential reworking or contamination, and were excluded from interpretation. Based on the remaining data, they proposed three earthquake events, including the 2002 rupture, with earlier events broadly constrained to pre-760 CE and post-1150 CE intervals.

While this pioneering work provides an important initial framework, its chronological resolution is limited by the small dataset and the use of decay counting techniques, which require larger samples and are more sensitive to contamination compared to Accelerator Mass Spectrometry (AMS) (e.g., Gove 1992; Bronk Ramsey et al. 2004; Hellborg and Skog 2008). In contrast, the present study employs AMS radiocarbon dating, allowing higher precision measurements on carefully selected samples and improved stratigraphic control. In addition, Bayesian modeling combined with sensitivity analyses demonstrates that all radiocarbon determinations are internally consistent, with no significant outliers and high convergence values. This confirms that the resulting chronology is robust and not influenced by individual samples. Despite methodological differences, the modeled ages obtained here (E3–E5) broadly overlap with the results of Akyüz et al. (2006), supporting the general timing of late Holocene earthquakes. However, the improved precision and reduced uncertainties achieved in this study provide a more reliable and quantitatively constrained earthquake history.

On the other hand, a comparable pattern is observed along the Simav Fault Zone within the ASFS, where trenching on the Sındırgı, Çaysimav, Şaphane, and Abide segments documents repeated Late Quaternary surface ruptures (Duman et al. 2013; Gürboğa 2013; Elmacı and Kürçer 2025). Identified events include multiple Holocene ruptures at Yeniköy and Ayvalı, four surface-faulting earthquakes in the Cüneyt area, one affecting late Holocene cultural horizons-and historical ruptures around AD 990 and 1020 on the Erdoğmuş Fault, with inferred recurrence intervals of ~900 years. These data confirm sustained activity of the ASFS extensional-transtentional system under the Western Anatolian stress regime. However, similar to the Çay Segment, the regional record does not indicate strictly periodic recurrence. Instead, earthquake occurrence is temporally irregular and distributed across adjacent fault strands.

Within this framework, the Çay Segment represents an integrated element of a kinematically linked normal-fault network. Its clustered late Holocene behavior likely reflects episodic strain release and inter-segment interaction rather than isolated, quasi-periodic rupture cycles. The 3 February 2002 Mw 6.5-6.0 sequence further attests to its continued activity under present-day extension. Overall, paleoseismic evidence supports episodic and spatially distributed surface faulting across the ASFS, favoring a clustered recurrence model over strictly periodic segment behavior.

GNSS measurements along the Akşehir-Simav Fault System document ongoing interseismic strain accumulation and suggest recurrence intervals of ~480–2360 year for $M > 6.5$ earthquakes. Segment-specific estimates further indicate shorter recurrence ranges of ~480–940 year for $M > 6.5$ events on the Sultandağı Fault, Işıklar Fault Zone, and Kali Çayı Fault Zone (Solak et al. 2026). Earlier geodetic studies further estimate extension rates of ~0.29 mm/yr (Aktuğ et al. 2009); assuming ~20–25 cm of vertical displacement per event,

this corresponds to a simplified long-term recurrence of ~ 1100–1200 year. While the shorter geodetic strain-based intervals are broadly consistent with the late Holocene recurrence pattern (E3-E5) derived from trench data, earlier periods reflect longer quiescent phases (Table 4). This discrepancy implies temporal clustering, variable segment interaction, or multi-segment ruptures within the fault system. Although only 23 year have elapsed since the 2002 surface-rupturing event, the occurrence of earthquake doublets in both 2002 and 2025 suggests that stress transfer and segment interaction play a key role in the evolving seismic hazard of the system.

5.3 Correlation with historical seismicity and magnitude estimation from surface rupture length along 2002 rupture

Historical sources document destructive earthquakes in AD 94 and/or AD 530 in the Afyon region (Ambraseys 2009) (Fig. 11; Table 5). According to his earthquake catalog, the AD 530 earthquake reportedly devastated the Phrygian cities of Polybotus (Bolvadin) and Philomelium. Although previous studies have associated these events with neighboring structures (e.g., Bolvadin Fault; Özkaymak et al. 2019), spatial uncertainties and limited macroseismic constraints prevent definitive source attribution. Comparison between modeled paleoseismic ages and historical records suggests that event E3 may correspond to either the historically documented earthquakes of AD 94 or AD 530, whereas event E5 unequivocally matches the 2002 Çay earthquake, which left a clear surface rupture in both trenches. However, given the width of the 95% credible intervals for E3 and the scarcity of reliable macroseismic intensity data, this correlation remains speculative. Definitive correlation would require complementary dating techniques, such as optically stimulated luminescence (OSL) dating, to refine the chronological framework. Future studies integrating multiple geochronological methods are needed to test these potential linkages and reduce chronological uncertainties.

Moreover, event E5, corresponding to the most recent surface-faulting earthquake in 2002, ruptured along the Çay segment of the Sultandağı Fault. The rupture length and its surface characteristics have been comprehensively documented by Emre et al. (2003). Using the surface rupture length we can estimated the earthquake and rupture length using the regression formula of Wells of Coppersmith 1994. In this equation, where M is moment magnitude, SRL is surface rupture length (km), and coefficients for normal faulting are $a = 4.86$ and $b = 1.32$.

The cumulative surface rupture length observed during the 2002 Çay earthquake sequence is approximately 26 km. Substituting this value yields:

Table 4 Event timing in the trenches along the Çay segment corresponding earthquakes and their elapsed times

Trench-event	%95.4–2 sigma-modeled with Oxcal	Correlated earthquakes	Elapsed time since the last surface rupture (yr)
E1	3635BC–2935BC	–	–
E2	2172BC–1656BC	–	
E3	1017BC–531AD	94 AD/530 AD	1931/1495
E4	880AD–1290AD	–	–
E5	1996AD–2003AD	2002 AD	23

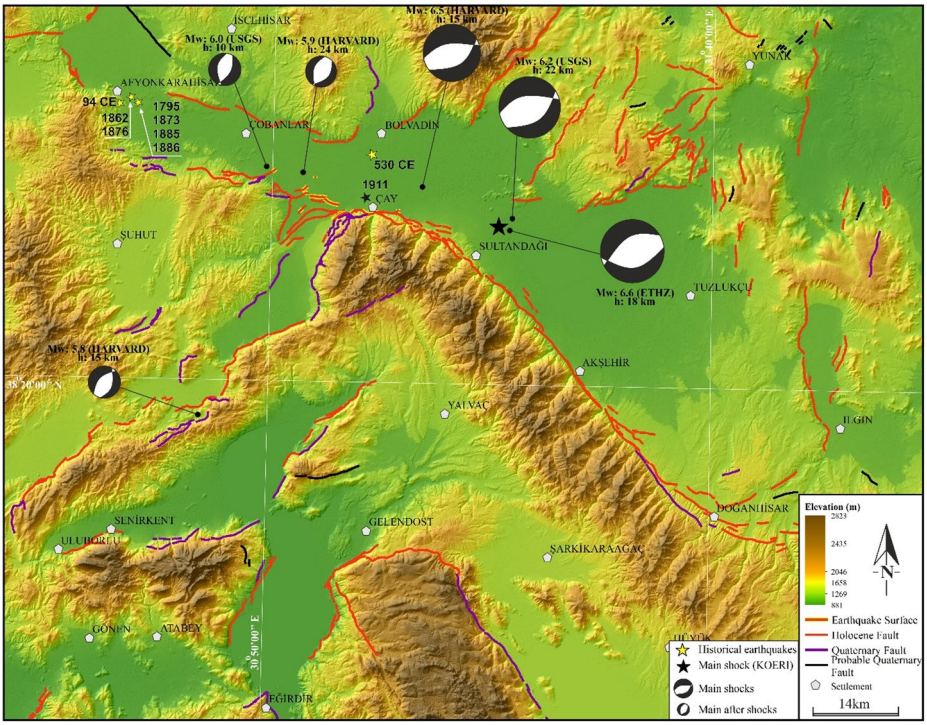

Fig. 11 Seismotectonic context of the study area illustrating the spatial distribution of the 2002 Çay earthquake and historically documented seismic events along the Akşehir Fault zone. Historical earthquake data are compiled from Ambraseys (2009) and Soysal et al. (1981)

Table 5 Historical earthquakes in the region, listed in their chronological order. Data compiled from Ambraseys (2009) and Soysal et al. (1981)

Event	Earthquake date (AD)	Location
1	94	Afyon
2	530	Polybotus
3	1766	Şuhut-Afyon
4	1795	Afyon
5	1862	Şuhut-Afyon
6	1873	Afyon
7	1876	Afyon
8	1897	Afyon

$M = 4.86 + 1.32\log(26)\ \log(26) = 1.41\ M \approx 6.72$ The resulting estimate (Mw≈6.7) is consistent with the instrumentally reported Mw 6.5, supporting the applicability of empirical scaling laws to the segment. Furthermore, the observed vertical displacements of ~20–25 cm in trench exposures are compatible with moderate normal-faulting events in the Mw 6–7 range.

In these scenarios using the equation; (i) the Çay segment is capable of generating Mw≥6.5 earthquakes in single-segment rupture scenarios. (ii) Measured paleo-displacements are consistent with empirical magnitude expectations. (iii) Multi-segment rupture scenarios could plausibly produce larger magnitudes, although such scenarios remain specu-

lative without additional structural evidence. Overall, the paleomagnitude (2002 Çay earthquake Mw 6.5) estimates are coherent with geodetic slip rates and observations from the 2002 event, strengthening the quantitative seismic hazard characterization of the segment.

5.4 Ground behavior, surface deformation, and implications for hazard mapping

The stratigraphic framework exposed in the trench walls reveals thick accumulations of unconsolidated Holocene lacustrine and alluvial deposits that play a critical role not only in preserving paleoearthquake evidence but also in controlling co-seismic and post-seismic ground behavior (e.g., Castro 1987; McGill and Sieh 1993; Audemard and Michetti 2011; Ishihara 2021). Such young, fine-grained to poorly consolidated sediments are particularly susceptible to seismic wave amplification, differential compaction, and secondary deformation processes (e.g., Seale and Archuleta 1989; Kozacı et al. 2011; Özaksoy et al. 2010). Consequently, local ground response conditions may significantly influence both the expression of surface rupture and the spatial distribution of earthquake damage.

During strong ground shaking, low-to-moderate shear-wave velocity (Vs30) sediments can amplify seismic waves, increase peak ground accelerations, and promote near-surface strain localization (e.g., Joyner and Fumal 1984; Joyner and Boore 1988; Ozcep et al. 2013). These processes may enhance the geomorphic visibility of surface ruptures while simultaneously increasing the likelihood of secondary effects such as surface cracking, localized subsidence, and liquefaction-related deformation (e.g., Ulusay and Kuru 2004; Kutoglu 2026b). Post-seismic reworking and compaction of unconsolidated deposits may further modify microtopography, potentially affecting the long-term preservation of rupture features observed in trench stratigraphy.

The empirical magnitude estimation derived from the Wells and Coppersmith (1994) surface rupture length relation ($Mw \approx 6.7$ for a total SRL of 26 km) represents a tectonic-scale parameterization of seismic potential. However, the realized impact of such an event is strongly modulated by near-surface sediment properties. Therefore, seismic hazard assessment should integrate both tectonic source characteristics (e.g., rupture length, displacement, recurrence interval) and local site effects.

The Bayesian modeling of event chronologies using OxCal at the 95.4% confidence level provides statistically robust recurrence intervals that can be directly incorporated into time-dependent hazard models (e.g., Şengöçmen Geçkin et al. 2022; Softa et al. 2023; Softa 2024a,b; Öncü et al. 2024). When combined with site-response considerations, these recurrence parameters allow for improved deformation hazard mapping. In particular, the following aspects should be incorporated into updated regional hazard frameworks: explicit delineation of surface rupture corridors based on trench-derived rupture width and cumulative displacement data; integration of recurrence interval probability distributions into probabilistic seismic hazard assessment (PSHA); inclusion of Vs30-based microzonation and sediment thickness variability into ground motion prediction modeling; consideration of potential segmentation effects and cumulative Holocene deformation in long-term hazard scenarios (e.g., Gülerce et al. 2017; Nas et al. 2020; Akkar et al. 2018; Softa 2024a; Uyanık et al. 2024).

Importantly, deformation hazard is not limited to primary fault rupture. In sedimentary basins characterized by thick Holocene sequences, distributed deformation and soil amplification may produce damage patterns extending beyond the mapped fault trace (e.g.,

Borcherdt 1994; Olsen 2000; Erdik et al. 2004; Wills and Clahan 2006). Therefore, hazard maps based solely on fault geometry may underestimate the spatial extent of risk.

Overall, the combined evaluation of paleoseismological data, empirical magnitude scaling, and site-response characteristics provides a more comprehensive framework for assessing seismic hazard. Incorporating ground behavior into deformation hazard mapping enhances the reliability of regional risk assessments and supports evidence-based planning and mitigation strategies (Erdik et al. 2004; Sesetyan et al. 2011; Pitilakis et al. 2013). Taken together, the interaction between tectonic rupture parameters and near-surface sediment properties demonstrates that seismic hazard cannot be evaluated solely on the basis of magnitude and recurrence statistics. Instead, deformation processes, site amplification potential, and stratigraphic controls must be incorporated into an integrated hazard framework. Such a framework directly informs land-use regulation, infrastructure resilience planning, and probabilistic risk modeling. Therefore, the paleoseismological and ground-response findings presented here extend beyond geological reconstruction and provide a scientific basis for evidence-based policy development and disaster risk reduction strategies, as discussed in the following section.

5.5 Policy and risk implications

The paleoseismological evidence presented in this study has direct implications for seismic hazard assessment, land-use planning, and disaster risk reduction strategies in the region (e.g., McCalpin 2009; UNISDR 2015; Pagani et al. 2020). The integration of Bayesian-modeled recurrence intervals (95.4% confidence level), empirical magnitude estimates based on surface rupture length, and stratigraphic evidence of Holocene ground deformation provides a robust framework for time-dependent seismic hazard evaluation (e.g., Wells and Coppersmith 1994; Parsons 2008; Biasi and Weldon 2009; McCalpin 2009).

The estimated moment magnitude of Mw ≈ 6.7 derived from the Wells and Coppersmith (1994) surface rupture length relation, together with recurrence intervals on the order of ~ 1 kyr, indicates that the Çay segment is capable of generating moderate-to-large surface-rupturing earthquakes with significant societal impact. Importantly, the presence of thick unconsolidated Holocene sediments suggests that ground motion amplification and secondary deformation (e.g., differential settlement, surface cracking, and potential liquefaction) may locally increase damage levels beyond what would be expected from magnitude alone (e.g., Ozcep et al. 2013; Ulusay and Kuru 2004; Akkar et al. 2018; Uyanık et al. 2024).

From a policy perspective, these findings highlight several priorities: (i) revision of active fault setback zones (e.g., Kerr et al. 2003; Christenson et al. 2003 Gökçe et al. 2014; Shirahama et al. 2016; Sözbilir et al. 2018), (ii) integration into probabilistic seismic hazard assessment (PSHA), (e.g., Cornell and Toro 1970; Field et al. 2015), (iii) microzonation and site-specific building codes (e.g., Erdik et al. 2004; Sesetyan et al. 2011; Pitilakis et al. 2013), (iv) early warning and real-time monitoring applications: risk-informed urban planning (Kumar et al. 2022; Sandeep and Huang 2025; Mittal et al. 2025; Pal et al. 2024, 2025).

Overall, this study demonstrates that paleoseismological data are not merely retrospective reconstructions of past earthquakes but constitute actionable inputs for contemporary risk management. Updating deformation hazard maps and integrating recurrence statistics into dynamic hazard frameworks will enhance regional resilience and support evidence-based disaster risk reduction policies in Türkiye.

6 Conclusions

This study integrates field studies, trench-based paleoseismology, Bayesian chronological modeling, historical earthquake comparison, and geodetic constraints to evaluate the Holocene behavior of the Çay segment of the Sultandağı Fault within the Akşehir-Simav Fault System. The main conclusions are:

- The Çay segment has experienced five Holocene surface-rupturing earthquakes, the youngest of which is the 2002 Mw 6.5 event.
- Recurrence intervals are variable, ranging from ~0.73 to ~1.16 kyr, with possible extensions up to ~1.59 kyr when uncertainties are considered.
- Individual earthquakes produce approximately 20–25 cm of vertical displacement, consistent with regional geodetic extension rates (~0.29 mm/year).
- The late Holocene record suggests temporal clustering rather than strictly periodic behavior.
- Correlation with historical earthquakes remains tentative due to limited macroseismic constraints, reinforcing the value of paleoseismic investigations in hazard assessment.

From a hazard perspective, the Akşehir-Simav Fault System (ASFS) behaves as an interacting extensional fault network capable of generating repeated Mw≥6 surface-rupturing earthquakes. The 2002 Çay earthquakes and the 2025 Sındırgı doublets demonstrate that seismic hazard is distributed along the entire system, not confined to isolated segments. These findings emphasize the necessity of incorporating paleoseismic recurrence variability, segment interaction, and slip-rate consistency into time-dependent probabilistic seismic hazard models for western Anatolia. Continued integration of high-resolution geomorphology, trench investigations, and geodetic monitoring will be essential for improving regional risk mitigation strategies.

Acknowledgements This study was conducted within the framework of a research project supported by the General Directorate of Mineral Research and Exploration (MTA). The authors gratefully acknowledge the MTA authorities for granting permission to publish this portion of the field results. This paper also constitutes part of the MSc thesis of Hasret Ozan Avcı. The authors further thank Selim Özalp for kindly allowing the use of field photographs documenting the surface ruptures produced by the 2002 Çay earthquake, captured shortly after the event. We also sincerely thank the four anonymous reviewers for their constructive comments and insightful suggestions, which significantly improved the quality of the manuscript.

Author contributions All authors contributed to the conception and design of the study. Material preparation, field investigations, data collection, and analyses were performed by Volkan Özaksoy, Hasan Elmacı, Hasret Ozan Avcı, and Mustafa Softa. Volkan Özaksoy prepared the first draft of the manuscript. All authors contributed to the interpretation of the results, critically revised earlier versions of the manuscript, and approved the final version for submission.

Funding Open access funding provided by the Scientific and Technological Research Council of Türkiye (TÜBİTAK). This study was supported by Mineral Research and Exploration (MTA), Ankara, Türkiye.

Data availability The active fault and seismotectonic database of Türkiye was compiled from Emre et al. (2018) and Duman et al. (2018). Selected maps were georeferenced and digitized using standard GIS workflows. Photomosaics, format conversions, and rectifications were performed using ArcGIS Pro (licensed through Dokuz Eylül University). Additional digital elevation model (DEM) products were retrieved from the Copernicus Data Space Ecosystem. All digital datasets were accessed in February 2026. Further, bayesian chronological modeling was performed using the OxCal program (v4.x), available at the Oxford Radiocarbon

Accelerator Unit (https://c14.arch.ox.ac.uk/oxcal.html). The processed data and results generated during this study are documented within the article. Additional datasets are available from the corresponding author upon reasonable request.

Declarations

Conflict of interest I declare that I have no conflicts of interest related to this project. This project was supported by General Directorate of Mineral Research and Exploration (MTA) under the Paleoseismology Project of Türkiye.

Open Access This article is licensed under a Creative Commons Attribution 4.0 International License, which permits use, sharing, adaptation, distribution and reproduction in any medium or format, as long as you give appropriate credit to the original author(s) and the source, provide a link to the Creative Commons licence, and indicate if changes were made. The images or other third party material in this article are included in the article's Creative Commons licence, unless indicated otherwise in a credit line to the material. If material is not included in the article's Creative Commons licence and your intended use is not permitted by statutory regulation or exceeds the permitted use, you will need to obtain permission directly from the copyright holder. To view a copy of this licence, visit http://creativecommons.org/licenses/by/4.0/.

References

Akgün E (2024) Kinematic and morphometric evidence for recent reactivation of the Kale-Yeşilyurt fault zone within the East Anatolian Fault System. J Mt Sci 21(12):4149–4176

Akgün E, Softa M (2025) 6 Şubat 2023 Mw 7.7 Pazarcık depremi: Çakmak Fayı (Adıyaman-Gölbaşı-Akçabel) boyunca yüzey kırığının karakteristik özellikleri. Gümüşhane Üniversitesi Fen Bilimleri Dergisi 15(3):653–666

Akgün E, Topal S, Softa M, Nas M, Gürgöze S, Sözbilir H, Yüksel M (2025) Evidence for an aseismic gap between the Mw6. 8 Pütürge (Elazığ) and 7.8 Pazarcık (Kahramanmaraş) earthquakes in the east Anatolian fault system, southeast Türkiye. J Struct Geol 190:105293

Akgün E, Softa M, Irfan M, Topal S (2026) Tectonic controls on active deformation and landscape evolution in the Amanos Mountains along the Düziçi–İskenderun Fault Zone, Eastern Anatolian Fault System. Prog Phys Geogr: Earth Environ. https://doi.org/10.1177/03091333261434479

Akkar S, Kale Ö, Yakut A, Ceken U (2018) Ground-motion characterization for the probabilistic seismic hazard assessment in Turkey. Bull Earthq Eng 16(8):3439–3463

Aksoy E, Akgün E, Softa M, Koçbulut F, Sözbilir H, Tatar O, Erol S Ç (2023) 6 Şubat 2023 Pazarcık (Kahramanmaraş) depreminin Doğu Anadolu Fay Zonu Erkenek ve Pazarcık Segmentleri Üzerindeki Etkisi: Çelikhan-Gölbaşı (Adıyaman) Arasından Gözlemler. Türk Deprem Araştırma Dergisi 5(1):85–104

Aktuğ B, Nocquet JM, Cingöz A, Parsons B, Erkan Y, England P, Tekgül A (2009) Deformation of western Turkey from a combination of permanent and campaign GPS data: Limits to block-like behavior. J Geophys Res: Solid Earth 114:B10

Aktuğ B, Tiryakioğlu I, Sözbilir H, Özener H, Özkaymak Ç, Yiğit CÖ, Softa M (2021) GPS derived finite source mechanism of the 30 October 2020 Samos earthquake, Mw = 6.9, in the Aegean extensional region. Turk J Earth Sci 30(8):718–737

Akyüz HS, Uçarkuş G, Şatır D, Dikbaş A, Kozacı Ö (2006) 3 Şubat 2002 Çay depreminde meydana gelen yüzey kırığı üzerinde paleosismolojik araştırmalar. Yerbilimleri 27(1):41–52

Ambraseys N (2009) Earthquakes in the Mediterranean and Middle East: a multidisciplinary study of seismicity up to 1900. Cambridge University Press

Atalay A (1975) Tektonik hareketlerin Sultandağın jeomorfolojisine olan etkileri [The effects of tectonic movements on the geomorphology of Sultandagı. Geol Soc Turk Bull 18:21–26

Audemard MFA, and, Michetti AM (2011) Geological criteria for evaluating seismicity revisited: forty years of paleoseismic investigations and the natural record of past earthquakes. In: Audemard MFA, Michetti AM, McCalpin JP (eds) Geological criteria for evaluating seismicity revisited: forty years of Paleoseismic investigations and the natural record of past earthquakes: geological society of America special paper, vol 479, pp 1–21 https://doi.org/10.1130/2011.2479(00)

Barka A, Reilinger R, Şaroğlu F, Şengör AMC (1995) The İsparta angle: its importance in the neotectonics of the Eastern Mediterranean Region. In: International earth sciences colloquium on the Aegean region, 9–14 October 1995, Proceedings, v.l, pp 3–17

Biasi GP, Weldon RJ (2009) San Andreas fault rupture scenarios from multiple paleoseismic records: stringing pearls. Bull Seismol Soc Am 99(2A):471–498

Blumenthal M (1963) Le syst_eme structural du Taurus sud-Anatolien. M_em. hors-s_erie Soc. geol. Fr., Livre _a la m_emoire du Professeur Paul Fallot, pp 611–662

Boray A, Şaroğlu F, Emre Ö (1985) Isparta Büklümünün kuzey kesiminde D-B daralma için bazı veriler (Evidence for E-W shortening in the north of Isparta Angle). Jeoloji Mühendisliği 23:9–20 (in Turkish with English abstract)

Borcherdt RD (1994) Estimates of site-dependent response spectra for design (methodology and justification). Earthq spectra 10(4):617–653

Bozkurt E, Rojay B (2005) Episodic, two-stage Neogene extension and short-term intervening compression in western Anatolia: field evidence from the Kiraz basin and Bozdağ horst. Geodin Acta 18(3–4):295–312

Bronk Ramsey C (1994) Analysis of Chronological Information and Radiocarbon Calibration: the Program OxCal. Archaeol Comput Newsl 41:11–16

Bronk Ramsey C (1995) Radiocarbon calibration and analysis of stratigraphy: the OxCal program. Radiocarbon 37(2):425–430

Bronk Ramsey C (2001) Development of the radiocarbon calibration program OxCal. Radiocarbon 43(2A):355–363

Bronk Ramsey C (2008) Deposition models for chronological records. Q Sci Rev 27(1–2):42–60

Bronk Ramsey C (2009) Bayesian analysis of radiocarbon dates. Radiocarbon 51(1):337–360

Bronk Ramsey C, Higham T, Leach P (2004) Towards high-precision AMS: progress and limitations. Radiocarbon 46(1):17–24. https://doi.org/10.1017/S0033822200039308

Castro G (1987) On the behavior of soils during earthquakes–liquefaction. Developments Geotech Eng 42:169–204

Christenson GE, Batatian LD, Nelson CV (2003) Guidelines for evaluating surface-fault-rupture hazards in Utah. Utah Geological Survey Miscellaneous Publication, Salt Lake City, pp 03–06

Cornell CA, Toro G (1970) Seismic Hazard Assessment. In: Hunter RL, Mann CJ (eds) International association for mathematical geology studies in mathematical geology, No. 4, techniques for determining probabilities of geologic events and processes. Oxford University Press, Oxford, pp 147–166

Demirtaş R, Iravul Y, ve Yaman M (2002) 3 Şubat 2002 Eber ve Çay depremleri ön raporu. Jeoloji Mühendisliği Haber Bülteni, 2002/1–2, 58–63

Dewey JF, Şengör AMC (1979) Aegean and surrounding regions: Complex multiplate and continuum tectonics in a convergent zone. Geol Soc Am Bull 90:84–92

Duman TY, Elmacı H, Özalp S, Olgun Ş, Emre Ö (2013) Simav Fay Zonunda İlk Paleosismolojik Bulgular; 66th geological congress of Turkey, Ankara, 1–5 April 2013, pp 28–29

Duman TY, Çan T, Emre Ö, Kadirioğlu FT, Baştürk NB, Kılıç T, Arslan S, Özalp S, Kartal RF, Kalafat D, Karakaya F, Azak TE, Özel NM, Ergintav S, Akkar S, Altınok Y, Tekin S, Cingöz A, Kurt Aİ (2018) Seismotectonics database of Turkey. Bull Earthq Eng. https://doi.org/10.1007/s10518-016-9965-9

Duran İ, Sözbilir H, Eski S, Softa M, Uytun H, Yüksel M, Topaksu M (2021) Paleoseismic history of the Manisa fault zone, Western Anatolia. Turkish J Earth Sci 30 8, Article 7. https://doi.org/10.3906/yer-2109-3

Elmacı H, Kürçer A (2025) 27 Ekim 2025 Sındırgı (Balıkesir) Depremi (Mw6,1) Bilgi Notu. MTA Raporu 2025. Available online: (accessed on 15 November 2025) https://www.mta.gov.tr/v3.0/sayfalar/bilgi-merkezi/deprem/pdf/Deprem_Bilgi%20Notu_2025-10%2027_Sindirgi_Balikesir_Depremi_Mw6.1.pdf

Emre T, Sozbilir H (2007) Tectonic evolution of the Kiraz Basin, Küçük Menderes Graben: evidence for compression/uplift-related basin formation overprinted by extensional tectonics in West Anatolia. Turkish J Earth Sci 16(4):441–470

Emre Ö, Duman TY, Doğan A, Özalp S, Tokay F, Kuşçu İ (2003) Surface faulting associated with the Sultandağı earthquake (M_w 6.5) of 3 February 2002, Southwestern Turkey. Seismol Res Lett 74(4):382–392 https://doi.org/10.1785/gssrl.74.4.382

Emre Ö, Duman TY, Özalp S, Olgun Ş, Elmacı H (2011) 1/250 000 Scale active fault map series of Türkiye, Afyon (NJ 36 – 5) Quadrangel Serial Number: 16, General Directorate of Mineral Research and Exploration. Ankara, Türkiye

Emre Ö, Duman TY, Özalp S, Şaroğlu F, Olgun Ş, Elmacı H, Çan T (2018) Active fault database of Turkey. Bull Earthq Eng 26:3229–3275

Erdik M, Demircioglu M, Sesetyan K, Durukal E, Siyahi B (2004) Earthquake hazard in Marmara region, Turkey. Soil Dyn Earthq Eng 24(8):605–631

Ertuncay D, Buyukakpinar P, Fornasari SF, Tan O (2025) 23 April 2025 Marmara Sea (Mw 6.3), Türkiye earthquake: mainshock, aftershock, and ground observations. Seismica 4(2)

Field EH, Biasi GP, Bird P, Dawson TE, Felzer KR, Jackson DD, Zeng Y (2015) Long-term time-dependent probabilities for the third Uniform California Earthquake Rupture Forecast (UCERF3). Bull Seismol Soc Am 105(2A):511–543

Geçkin BŞ, Sözbilir H, Özkaymak Ç, Softa M, Spencer JQ, Şahiner E, Deliormanlı AH (2022) Evidence of surface rupture associated with historical earthquakes on the Gülbahçe Fault Zone (İzmir, Türkiye) and its application for determination of the surface fault-rupture hazard zone. Nat Hazards 114(2):2189–2218

Gökçe O, Tüfekçi MK, Gürboğa Ş (2014) Evaluation of surface faulting hazard and creation of fault avoidance zone. Prime ministry of disaster and emergency management. pp 384

Gove HE (1992) The History of AMS, its Advantages over Decay Counting: Applications and Prospects. In: Taylor RE, Long A, Kra RS (eds) Radiocarbon After Four Decades. Springer, New York, NY. https://doi.org/10.1007/978-1-4757-4249-7_15.

Gülerce Z, Tanvir Shah S, Menekşe A, Arda Özacar A, Kaymakci N, Önder Çetin K (2017) Probabilistic seismic-hazard assessment for East Anatolian fault zone using planar fault source models. Bull Seismol Soc Am 107(5):2353–2366

Gürboğa Ş (2013) 28 March 1970 Gediz earthquake fault, western Turkey: palaeoseismology and tectonic significance. Int Geol Rev 55(10):1191–1201

Gürer A, Bayrak M, Gürer ÖF, Ilkişik OM (2004) The deep resistivity structure of southwestern Turkey: tectonic implications. Int Geol Rev 46(7):655–670

Güvercin SE, Karabulut H, Konca AÖ, Doğan U, Ergintav S (2022) Active seismotectonics of the East Anatolian fault. Geophys J Int 230(1):50–69

Hellborg R, Skog G (2008) Accelerator mass spectrometry. Mass Spectrom Rev 27:398–427. https://doi.org/10.1002/mas.20172

Hua Q, Turnbull JC, Santos GM, Rakowski AZ, Ancapichún S, De Pol-Holz R, Turney CS (2022) Atmospheric radiocarbon for the period 1950–2019. Radiocarbon 64(4):723–745

Ishihara K (2021) Evaluation of soil properties for use in earthquake response analysis. Geomechanical modelling in engineering practice. Routledge, pp 241–275

Joyner WB, Boore DM (1988) Measurement, characterization, and prediction of strong ground motion. In: Earthquake engineering and soil dynamics II, Proc. Am. Soc. Civil Eng. Geotech. Eng. Div. Specialty Conf, pp 27–30

Joyner WB, Fumal TE (1984) Use of measured shear-wave velocity for predicting geologic and site effects on strong ground motion. In: Proc 8th world conference on earthquake engineering, 2:777–783

Karabacak V, Özkaymak Ç, Sözbilir H, Tatar O, Aktuğ B, Özdağ ÖC, Arslan G (2023) The 2023 Pazarcık (Kahramanmaraş, Türkiye) earthquake (Mw 7.7): Implications for surface rupture dynamics along the East Anatolian fault zone. J Geol Soc 180(3):jgs2023–jgs2020

Kerr J, Nathan S, Van Dissen R et al (2003) Planning for development of land on, or close to active faults: an interim guideline to assist resource management planners in New Zealand. Inst Geol Nucl Sci Client Rep 124:52

Koçyiğit A (2005) The Denizli graben-horst system and the eastern limit of western Anatolian continental extension: basin fill, structure, deformational mode, throw amount and episodic evolutionary history, SW Turkey. Geodin Acta 18(3–4):167–208

Koçyiğit A, Deveci Ş (2007) A NS-trending active extensional structure, the Şuhut (Afyon) graben: commencement age of the extensional neotectonic period in the Isparta Angle, SW Turkey. Turkish J Earth Sci 16(4):391–416

Koçyiğit A, Özacar A (2003) Extensional neotectonic regime through the NE edge of the outer Isparta Angle, SW Turkey: new field and seismic data. Turkish J Earth Sci 12(1):67–90

Koçyiğit A (1984) Tectono-stratigraphic characteristics of Hoyran Lake region (Isparta Bend). In: Geology of the Taurus Belt – proceedings of international tauride symposium, Tekeli O, Göncüoğlu MC (eds), pp 53–67. Mineral Research and Exploration Institute of Turkey (MTA), Ankara

Koçyiğit A, Ünay E, Saraç G (2000) Episodic graben formation and extensional neotectonic regime in west Central Anatolia and the Isparta Angle: a case study in the Akşehir-Afyon Graben, Turkey. In: Bozkurt E, Winchester JA, Piper JDA (eds), Tectonics and magmatism in Turkey and the surrounding area. Geological Society, London, Special Publications 173, pp 405–421

Kozaci Ö, Altunel E, Lindvall S, Brankman C, Lettis W (2011) The North Anatolian fault on the Hersek Peninsula, Turkey: Its geometry and implications for the 1999 Izmit earthquake rupture propagation. Turkish J earth Sci 20(4):359–378

Kumar R, Mittal H, Sandeep A, Sharma B (2022) Earthquake genesis and earthquake early warning systems: challenges and a way forward. Surv Geophys 43(4):1143–1168

Kürçer A, Özalp S, Özdemir E, Uygun Güldoğan Ç, Duman TD (2016) Yüzey Kırığı Oluşturmuş Faylar Üzerinde Aktif Tektonik ve Paleosismoloji Araştırmalar Hakkında Örnek Çalışma: Yenice Gönen Fayı, KB Türkiye. MTA Doğal Kaynaklar ve Ekonomi Bülteni, pp 1–18

Kutoğlu ŞH, Softa M, Akgün E, Nas M, Topal S (2026a) Analyzing Fault reactivation behavior using InSAR, stress inversion, and field observations during the 2025 Sındırgı earthquake sequence, Simav Fault Zone, Western Türkiye. Sensors 26(3):760
Kutoğlu ŞH, Akgün E, Softa M (2026b) Delineating the Central Anatolia Transition Zone (CATZ): constraints from integrated geodetic (GNSS/InSAR) and seismic data. Sensors 26(2):505
McCalpin JP (2009) Paleoseismology in extensional tectonic environments. Int Geophys 95:171–269
McGill S, Sieh K (1993) Holocene slip rate of the central Garlock fault in southeastern Searles Valley, California. J Geophys Res Solid Earth 98(B8):14217–14231
McKenzie D (1972) Active tectonics of the Mediterranean region. Geophys J Roy Astron Soc 30:109–195
Mittal H, Pal S, Kumar R, Saini A, Wu YM, Ammani A, Mishra OP (2025) India's earthquake early warning systems: a review of developments and challenges. Surv Geophys 46(3):529–553
Nas M, Lyubushin A, Softa M, Bayrak Y (2020) Comparative PGA-driven probabilistic seismic hazard assessment (PSHA) of Turkey with a Bayesian perspective. J Seismolog 24(6):1109–1129
Öcal H, Alan İ, Balcı V, Keskin H (2011a) 1:100.000 ölçekli Türkiye Jeoloji Haritaları No: 160 Afyon-K26 Paftası. MTA, Ankara, No, p 160
Öcal H, Turhan N, Göktaş F, Ankara (2011b) 1:100.000 ölçekli Türkiye Jeoloji Haritaları No: 259 Afyon – K25 Paftası. MTA, Ankara, No:259
Olsen KB (2000) Site amplification in the Los Angeles basin from three-dimensional modeling of ground motion. Bull Seismol Soc Am 90(6B):S77–S94
Öncü U, Sözbilir H, Özkaymak Ç, Softa M, Sümer Ö, Eski S, Topaksu M (2024) Palaeoseismological assessment for a seismic gap located very close to the epicentre of the 30 October 2020 Samos Earthquake (M6. 9), western Anatolia, Turkey. Nat Hazards 120(5):4699–4727
Özaksoy V, Emre Ö, Yıldırım C, Doğan A, Özalp S, Tokay F (2010) Sedimentary record of late Holocene seismicity and uplift of Hersek restraining bend along the North Anatolian Fault in the Gulf of İzmit. Tectonophysics 487(1–4):33–45
Ozcep T, Ozcep F, Ozel O (2013) VS30, site amplifications and some comparisons: the Adapazari (Turkey) case, vol 63. In: Physics and chemistry of the earth, Parts A/B/C, pp 92–101
Özden S, Kavak KS, Koçbulut F, Över S, Temiz H (2002) 3 Şubat 2002 Çay (Afyon) depremleri. Türkiye Jeoloji Bülteni 45(2):49–56
Özgül N (1976) Some geological aspects of the Taurus orogenic belt. Bull Geol Soc Turk 19:65–78
Özgül N, Bölükbasi S, Alkan H, Öztas Y, Korucu M (1991) Tectonostratigraphic units of the Lake District, Western Taurides, Tectonics and hydrocarbon potential of Anatolia and surrounding regions. In: Ozan Sungurlu symposium proceedings, Ankara, pp 213–237
Özkaymak Ç, Sözbilir H, Geçievi MO, Tiryakioğlu İ (2019) Late Holocene coseismic rupture and aseismic creep on the Bolvadin Fault, Afyon Akşehir Graben, Western Anatolia. Turkish J Earth Sci 28(6):1. https://doi.org/10.3906/yer-1906-13
Pagani M, Garcia-Pelaez J, Gee R, Johnson K, Poggi V, Silva V, Weatherill G (2020) The 2018 version of the global earthquake model: hazard component. Earthq Spectra 36(1suppl):226–251
Pal SK, Sandeep, Gangajali S, Kumar P, Mittal H (2024) Development of region specific earthquake early warning scaling relations for the Garhwal region using observed and simulated datasets: a step forward to disaster mitigation. Bull Earthq Eng 22(8):3875–3904
Pal SK, Devi S, Kumar P, Joshi A, Kumar R (2025) Real-time earthquake magnitude estimation utilizing a mixed dataset set of observed and simulated P-wave onsets for the Kumaon Himalaya from Mw3. 0–7.5 earthquakes. In: Physics and Chemistry of the Earth, Parts A/B/C, p 104044
Parsons T (2008) Earthquake recurrence on the south Hayward fault is most consistent with a time dependent, renewal process. Geophys Res Lett 35(21)
Pitilakis K, Riga E, Anastasiadis A (2013) New code site classification, amplification factors and normalized response spectra based on a worldwide ground-motion database. Bull Earthq Eng 11(4):925–966
Reilinger R, McClusky S, Vernant P, Lawrence S, Ergintav S, Cakmak R, Karam G (2006) GPS constraints on continental deformation in the Africa-Arabia-Eurasia continental collision zone and implications for the dynamics of plate interactions. J Geophys Res Solid Earth 111:B5
Reimer PJ, Baillie MGL, Bard E, Bayliss et al (2009) IntCal09 and Marine09 radiocarbon age calibration curves, 0–50,000 years cal BP. Radiocarbon 51(4):1111–1150
Reimer PJ, Austin WE, Bard E, Bayliss A, Blackwell PG, Ramsey CB, Talamo S (2020) The IntCal20 Northern Hemisphere radiocarbon age calibration curve (0–55 cal kBP). Radiocarbon 62(4):725–757
Sandeep, Huang Y (2025) Development of earthquake early warning scaling relations for the Northeast India using observed and simulated datasets from Mw 6.1–8.3 earthquakes. Nat Hazards 121(9):10355–10376
Şaroğlu F, Emre Ö, Boray A (1987) Türkiye'nin Diri Fayları ve Depremselliği (Seismicity and Active Faults of Turkey). General Directorate of Mineral Research and Exploration (MTA) Report No. 8174 (in Turkish, unpublished)

Şaroğlu F, Emre Ö, Kuşçu İ (1992) Active Fault Map of Turkey. Maden Tetkik ve Arama (MTA) Enstitüsü, Ankara
Scharer K, McPhillips D, Leidelmeijer J, Kirby M (2024) Inbuilt age, residence time, and inherited age from radiocarbon dates of modern fires and late Holocene deposits, Western Transverse Ranges, California. Earth Surf Proc Land 49(8):2552–2566
Seale SH, Archuleta RJ (1989) Site amplification and attenuation of strong ground motion. Bull Seismol Soc Am 79(6):1673–1696
Şengör AMC (1979) The North Anatolian Transform Fault: its age, offset and tectonic significance. J Geol Soc Lond 136:269–282
Şengör AMC, Görür N, Şaroglu F (1985) Strike-slip faulting and related basin formation in zones of tectonic escape: Turkey as a case study. In: Biddle KT, Christie-Blick N (eds) Strike-Slip Deformation, Basin Formation, and Sedimentation, Spec Publ Soc Econ Paleontol Mineral 37:227–264
Sesetyan K, Zulfikar C, Demircioglu M, Hancilar U, Kamer Y, Erdik M (2011) Istanbul earthquake rapid response system: methods and practices. Soil Dyn Earthq Eng 31(2):170–180
Shirahama Y, Yoshimi M, Awata Y et al (2016) Characteristics of the surface ruptures associated with the 2016 Kumamoto earthquake sequence, central Kyushu, Japan. Earth Planet Space 68(1):1–12. https://doi.org/10.1186/s40623-016-0559-1
Softa M (2022) Morphometric and kinematic analysis of southern margin of the Küçük Menderes Graben and its tectonic implications in western Anatolia. Arab J Geosci 15(2):131
Softa M (2024a) Determining the surface fault-rupture hazard zone for the Pazarcık segment of the East Anatolian fault zone through comprehensive analysis of surface rupture from the February 6, 2023, Earthquake (Mw 7.7). J Mt Sci 21(8):2646–2663
Softa M (2024b) Unravelling the Pleistocene to Holocene earthquake chronology of the Seferihisar Fault, western Turkey: A comprehensive analysis using optically stimulated luminescence (OSL) dating and palaeoseismology. J Earth Syst Sci 133(4):225
Softa M, Şahiner E, Sözbilir H, Spencer JQ, Utku M, Büyüktopcu MF (2023) The first application of the luminescence surface exposure dating method on active fault scarps in the Western Anatolia extensional province: The Manisa Fault as an example. Turkish J Earth Sci 32(2):163–180
Softa M, Koçbulut F, Akgün E, Aksoy E, Sözbilir H, Tatar O, Arslan G (2024) Surface rupture during the 6th of February 2023 Mw 7.6 Elbistan-Ekinözü (Kahramanmaraş) earthquake: implications for fault rupture dynamics along the northern branch of East Anatolian Fault Zone. Turkish J Earth Sci 33(1):1–21
Solak Hİ, Tiryakioğlu İ, Özkaymak Ç, Gezgin C, Özyildirim Ö, Çakanşimşek EB, Aladoğan K (2026) Geodetic Analysis of Seismic Behavior in the Afyon-Akşehir Graben, western Anatolia. J Afr Earth Sci 106066
Soysal H, Sipahioğlu S, Kolçak D, Altınok Y (1981). Türkiye ve Çevresinin Tarihsel Deprem Kataloğu. TÜBİTAK Project No. TBAG 341, İstanbul, 86 pp.
Sözbilir H, Ozkaymak C, Uzel B et al (2018) Criteria for surface rupture microzonation of active faults for earthquake hazards in urban areas, N. Handbook of research on trends and digital advances in engineering geology, IGI Global 765. https://doi.org/10.4018/978-1-5225-2709-1
Tiryakioğlu İ, Özkaymak Ç, Baybura T, Sözbilir H, Uysal M (2018) Comparison of palaeostress analysis, geodetic strain rates and seismic data in the western part of the Sultandagi fault in Turkey. Ann Geophys 61(3)
Topal S, Softa M (2023) Geomorphic signature of active tectonics in Simav Graben: An evaluation of indicator relative tectonic activity of Simav Fault and its seismotectonic implications for Western Anatolia. J Earth Syst Sci 132(3):95
Topal S, Keller E, Bufe A, Koçyiğit A (2016) Tectonic geomorphology of a large normal fault: Akşehir fault, SW Turkey. Geomorphology 259:55–69
Ulusay R, Kuru T (2004) 1998 Adana-Ceyhan (Turkey) earthquake and a preliminary microzonation based on liquefaction potential for Ceyhan Town. Nat Hazards 32(1):59–88
UNISDR (United Nations International Strategy for Disaster Reduction) (2015) Sendai framework for disaster risk reduction 2015–2030. http://www.wcdrr.org/uploads/Sendai_Framework_for_Disaster_Risk_Reduction_2015-2030.pdf
Uyanık O, Öncü Z, Uyanık NA, Ekin N (2024) Seismic microzonation and geotechnical modeling studies considering local site effects for İnegöl Plain (Bursa-Turkey). Earth Space Sci 11(11):e2023EA003460
Uzel B, Langereis CG, Kaymakci N, Sözbilir H, Özkaymak Ç, Özkaptan M (2015) Paleomagnetic evidence for an inverse rotation history of Western Anatolia during the exhumation of Menderes core complex. Earth Planet Sci Lett 414:108–125
Wells DL, Coppersmith KJ (1994) New empirical relationships among magnitude, rupture length, rupture width, rupture area, and surface displacement. Bull Seismol Soc Am 84(4):974–1002
Wills CJ, Clahan KB (2006) Developing a map of geologically defined site-condition categories for California. Bull Seismol Soc Am 96(4A):1483–1501

Yeniyol M (1979) Yunak (Konya) manyezitlerinin oluşumu sorunları, değerlendirmeleri ve yöre kayaçlarının jeolojisi (Doctoral dissertation, Istanbul University, Institute of Science)

Publisher's note Springer Nature remains neutral with regard to jurisdictional claims in published maps and institutional affiliations.

Authors and Affiliations

Volkan Özaksoy[1] · Hasan Elmacı[2] · Hasret Ozan Avcı[2] · Mustafa Softa[3]

✉ Volkan Özaksoy
volkano@akdeniz.edu.tr

Hasan Elmacı
hasan.elmaci@mta.gov.tr

Hasret Ozan Avcı
hasret.avci@mtaic.gov.tr

Mustafa Softa
mustafa.softa@deu.edu.tr

[1] Faculty of Engineering, Department of Geological Engineering, Akdeniz University, 07058 Konyaaaltı, Antalya, Turkey

[2] General Directorate of Mineral Research and Exploration, Directorate of Geological Studies, 06800 Çankaya, Ankara, Turkey

[3] Faculty of Engineering, Department of Geological Engineering, Dokuz Eylül University, 35390 Izmir, Turkey